HOMOGENIZATION AND UNCERTAINTY ANALYSIS FOR FIBER REINFORCED COMPOSITES

By

JINUK KIM

A DISSERTATION PRESENTED TO THE GRADUATE SCHOOL
OF THE UNIVERSITY OF FLORIDA IN PARTIAL FULFILLMENT
OF THE REQUIREMENTS FOR THE DEGREE OF
DOCTOR OF PHILOSOPHY

UNIVERSITY OF FLORIDA

2011

To my Lord, parents, brother and friends

ACKNOWLEDGMENTS

I would like to sincerely thank Professor Nam-Ho Kim, for his impeccable guidance, understanding and patience throughout this work. His mentorship and encouragement have provided me with great excitement throughout the entire research life at the University of Florida. It was his direction, insight and criticism that lead me to the better way of research and study.

I express my gratitude to the members of my supervisory committee, Professor Susan Sinnott, Professor Anthony Brennan, Professor Simon Phillpot, Professor Elliot Douglas and Professor Youping Chen for their willingness to review my Ph.D. research and provide constructive comments to help me complete this dissertation.

Special thanks to Professor Susan Sinnott for her kind and thoughtful support as an advisor in materials science and engineering department.

I would also like to thank all my lab colleagues and friends in the materials science and engineering department and the MDO lab in MAE department.

Most importantly, I express my deep gratitude and thanks to my loving family. My father and mother have supported me throughout the school year with devotion and love. My brother has continuously prayed for me and showed me the right way to live by his every life and showed me the way to follow God’s footsteps and live a righteous life.

Finally, and most of all, I thank my Father in heaven for supporting my dreams and ambitions and forgiving me wrongdoings. Thank you and love you. You gave me all.

TABLE OF CONTENTS

LIST OF TABLES

LIST OF FIGURES

Abstract of Dissertation Presented to the Graduate School
of the University of Florida in Partial Fulfillment of the
Requirements for the Degree of Doctor of Philosophy

HOMOGENIZATION AND UNCERTAINTY ANALYSIS FOR FIBER REINFORCED COMPOSITES

By

Jinuk Kim

August 2011

Chair: Susan Sinnott
Cochair: Nam Ho Kim
Major: Materials Science and Engineering

Because of the geometrical complexity and multiple material constituents, the behavior of fiber reinforced composites is nonlinear and difficult to model. These complex and nonlinear behavior makes the computational cost much higher than that of general homogeneous materials. To make use of computational advantage, homogenization method is applied to the fiber reinforced composite model to minimize the cost at the expense of detail of local micro scale phenomena. It is nearly impossible to make a homogenized model that behaves exactly the same as the composites in every aspect. However, it would be worthwhile to use it when overall or specific macroscopic behavior is a major concern, such as overall heat flux in a given area, overall conductivity or overall stress level in a beam instead of microscopic accuracy. In this research, the effective stiffness matrix is calculated using homogenization of elastic behavior. In this case, the homogenization method was applied to the representative volume element (RVE) to represent elastic behavior. For homogenization of inelastic material, the anisotropic Ramberg-Osgood model is applied and its parameters are

calculated using the effective stress and effective strain relation obtained from the heterogeneous material analysis.

Many conventional structural analyses have been carried out on the basis of constant values for mechanical properties, including Young's modulus, Poisson ratio, heat capacity and so on. It means uncertainty in the material parameters is ruled out and while it is widely accepted, there is uncertainty and it is inevitable in the procedure of obtaining the values and even during the design process. This research applied the uncertainty analysis technique which makes use of a statistical approach such as stochastic response surface method (SRSM), to the behavior of the composite material. The main purpose of applying the uncertainty analysis is to see how the uncertainty in mechanical properties propagates to the macro behavior of the entire composites. Uncertainty in some properties could vanish away to the macro behavior and others can result in amplification or decrease of the uncertainty in macro behavior. Utilizing this analysis, design parameters that are important can be identified, which can help make an effective approach in development, design, or manufacturing processes.

CHAPTER 1
INTRODUCTION

Composite Analysis

Composite materials are macroscopically composed of more than two materials. A narrow definition of composites is restricted to combinations of materials that contain high strength fiber reinforcement and matrix that supports fiber [1]. As science and technology advance, the demand of high performance materials has been increased and its superior properties over single component systems have made the application of fiber reinforced composites popular in the industry. For structural applications, the greatest advantage of composites may come from high stiffness and strength per weight. Inexpensive fiberglass reinforced plastic composites have been used in various industrial and consumer products from automotive and aircraft since the 1950's [2]. Commercial airplane companies also provide a market for advanced composites application. The Boeing 787 makes great use of composite materials in its airframe and primary structure than any previous commercial airplanes. When the cost is not the main issue, such as military systems, advanced composites have been used more extensively. Not only jet fighters but also military vehicles feature integrated composite armored body.

Application of advanced composite materials for structures has continued to increase, but one of the biggest factors that limit the widespread application is their high cost in manufacturing process compared to conventional metallic alloy systems [3]. The high cost of composites manufacturing partially comes from the trial-and-error approach in design, process development and labor-intensive manufacturing process. It is due in

part to the complex geometry and mechanical and thermal characteristics of composites.

There are many different manufacturing processes for composites. Because of its relatively high ductility, thermoplastic is one of the famous materials used for the matrix part. Thermoplastic composites are supplied in a variety of ready to use intermediate forms, which is generally called prepreg, as shown in Figure 1-1. They can easily be controlled and processed through the standard production techniques [4].

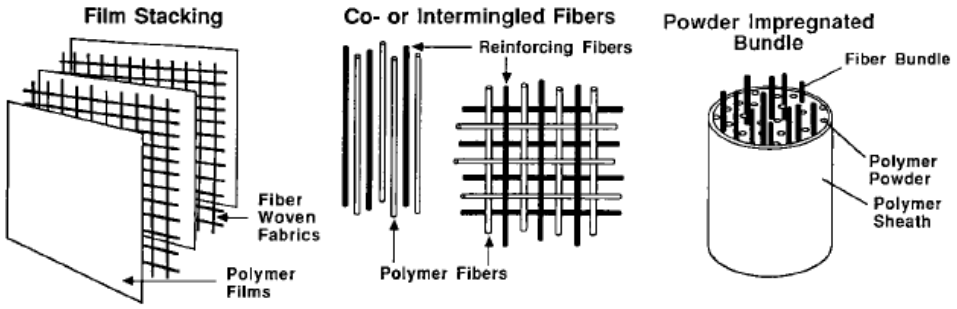

Figure 1-1. Intermediate material forms for thermoplastic composites.

When the behavior of composite structure is expected to be in elastic in working condition, such as automotive or aircraft working condition, plasticity could not be the main area of interest. But, it becomes a main issue in manufacturing process where composite materials experience plastic deformation. The product processes that are currently being used in industry are basically adapted from sheet metal forming processes. Production techniques for thermoplastic such as roll forming, pultrusion, compression molding, diaphragm forming, and stamp forming are similar to general metal forming processes. Figure 1-2 shows a schematic stamping forming process for the intermediate composite form. Since the purpose of this process is to produce permanent deformation to the material, it is called plasticity in the classical mechanics.

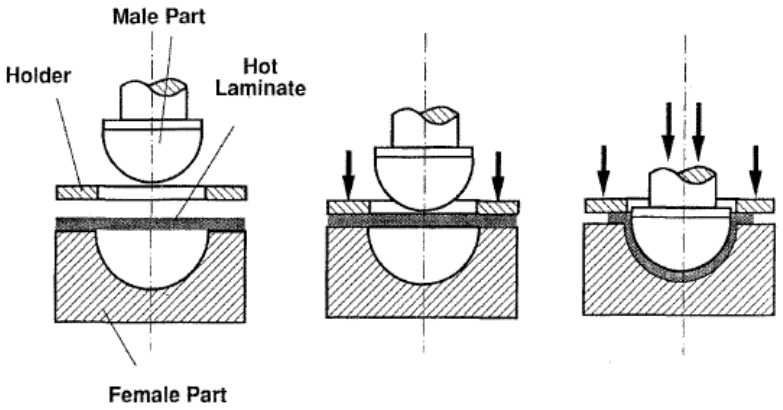

Figure 1-2. Stamp forming of thermoplastic composites.

Because of the high complexity of both material behavior and structural geometry, it is difficult to predict the production process. Therefore, it is essential to utilize numerical approaches to understand and predict the behavior of heterogeneous materials. The computational model and the prediction of the process require understandings of stress-strain relations of the heterogeneous materials. However, if heterogeneous materials are modeled directly using a full scale simulation, they requires too much computational source because they are usually very small features compared to the size of structures.

The classical plasticity theory is the most popular approach to model inelastic behavior and widely being used in many applications. But it requires too many parameters and complexity. This classical plasticity theory is reasonable for homogeneous or isotropic materials, but not for heterogeneous, anisotropic yielding, and anisotropic hardening materials at least. It has to contain more parameters and complex analytical expressions and more iteration to solve nonlinear equations leading to a great amount of computational cost and still having questions on accuracy.

The purpose of computational model is to predict the response of a structure accurately, which requires using proper model parameters. However, choosing model parameters for composites application have relied much on engineer's experience [5]. In addition, experiments showed that most structural parameters have random, stochastic characteristics. When the effect of these uncertainties in parameters is understood, the analysis and design process to develop advanced composite materials can have benefit from it by giving more accurate and reliable results. If critical parameters can be identified, detailed or optimized design can be possible by paying more attention on that critical parameter's effect. The process of estimating the effect of model parameter uncertainty on the response uncertainty is called uncertainty propagation. Accordingly, many probabilistic approaches have been introduced to predict more accurate behavior of system under uncertainty, and they showed the random character play a very important role in the decision making process. It seems that the random characteristic of heterogeneous materials would be more important than that of homogeneous materials.

For statistical approaches to engineering problems, the most popular method for uncertainty propagation analysis is Monte Carlo Simulation (MCS). The MCS method is one of the sampling methods, which generates random samples according to the probability distribution of random parameters, and using physical model to calculate the random samples of response. This method has an advantage of simplicity, which can be applicable to virtually all engineering applications, and the accuracy of the method is independent of the number of model parameters. However, in order to estimate the distribution of response accurately, a large number of samples are required, which is

equivalent to a numerous evaluation of the physical model. For modern advanced computational models, this can be a significant bottleneck as they requires significant amount of computational resources.

Motivation

For simulation of composite structures, using homogenization and a simpler material model than the classical plasticity theory can reduce computational cost significantly. It is virtually impossible to make a homogeneous material that behaves exactly same as heterogeneous materials in every aspect and scale. However, when a specific behavior is of interest, a homogenized material can be modeled so that it can have similar behavior under a limited condition. For example, when the temperature on the surface of heat barrier that is made of composite structure is the main interest, a homogeneous material that has the same or similar thermal property can replace the heterogeneous part. The same analogy can be applied to the constitutive model that defines the relation between stress and strain. Although, homogenization of elastic properties has been studied intensively by many researchers, not much research has been reported for homogenization of inelastic properties. Most of inelastic homogenization research is based on the classical plasticity theory, which requires many parameters to be defined, and consequently, leaving assumptions that cannot be used for heterogeneous materials, e.g., isotropic hardening. Therefore, more effective homogenization model than the classical one needs to be developed to make a good use of computational tools.

Although MCS is widely used, it becomes impractical for computationally expensive models because it requires a large number of samples, and each sample means evaluating the expensive computational model. Performing 50,000 finite element

analyses using input values generated by MCS for composite material is far beyond current computational ability especially when nonlinear behavior is considered. Although there are many approximation methods to improve computational cost, all of them introduce some kind of approximation, such as linearization. Therefore, it would be desirable to make the MCS sampling computationally inexpensive.

The complexity in modeling inelastic behavior using plasticity theory prevents not only the homogenization process, but also the statistical study because the statistical application still requires a significant amount of simulations. In addition, when geometric parameters are included, such as the size of fiber, it would be difficult to take into account their effect using the classical plasticity model. Because of these reasons, uncertainty analysis on inelastic behavior has difficulty in application for heterogeneous materials.

Objective

The first objective of this research is to develop a homogenization methodology for unidirectional fiber reinforced composites by using numerical method so that the homogenized material model can provide the same effective stress-strain relation in macroscopic scale as heterogeneous materials. For the elastic behavior, effective stiffness components or effective elastic properties such as effective Young's modulus are to be calculated. For inelastic behavior, the composites is considered as elastoplastic materials and is to be homogenized through the Ramberg-Osgood model with anisotropy tensor imbedded in, which reduces significantly the number of plasticity parameters and numerical iterations. Throughout this research, representative volume element (RVE) and unit volume element (UVE) are to be used to understand the behavior of composites and homogenize the heterogeneous materials more accurately.

The periodic boundary condition that assigns the periodicity to RVE model is also discussed for its validity.

The second objective of this research is to perform uncertainty analysis using stochastic response surface method (SRSM) that uses more efficient sampling method than Monte Carlo Simulation. The uncertainty analysis is performed not only for elastic properties but also for inelastic properties. The homogenized material with a simpler material model enables the uncertainty analysis for inelastic behavior. From the uncertainty analysis, the focus is given on how much uncertainties that exist in mechanical or geometrical properties propagate into the macroscopic behavior of the composites. Consequently, it gives information on which parameters are critical in a given specific conditions so that composites development, design and manufacturing process can have benefits from the analysis.

CHAPTER 2
LITERATURE REVIEW

Homogenization

Almost all structural materials are heterogeneous in micro- and/or macro-scale. It is generally known that the macro-scale behavior of a structure is caused by the micro-scale behavior. The micro-scale behavior is often more complicated than that of the macro-scale. In fiber-reinforced composites, for example, the inhomogeneous local displacement field can be developed even under uniform global displacement. In such a case, it would be necessary to have a micro-scale model in order to describe this local behavior. However, because of limited computational resources and modeling complexity, it would be impractical to perform all-in-one analysis for composite structure from the micro-scale to the macro-scale [7]. Instead of full scale analysis, when effective properties of the composite materials are used by averaging the local behavior of individual fibers and matrices [8], the composite structure can be modeled as a homogeneous material in the macro-scale considering only effective properties.

Among numerous methods to predict the effective properties of composite materials, a variety of theories have been developed for homogenization, such as effective medium models of Eshelby [9], Hashin [10], and Mori and Tanaka [11]. The simple bounds on the effective moduli can be determined by the approaches of Voigt [12] and Reuss [13]. From a different perspective, Hill [14] and Christensen [15] proposed a self consistent method. Hill [16] also showed that Voigt and Reuss approaches provide rigorous upper and lower bounds, respectively. Mathematical or analytical homogenization methods had been pioneered by Bensoussan [17] and Sanchez-Palencia [18]. The active computational aspects of homogenization have been

initiated by Guedes and Kikuchi [19]. Over the past decade major contributions have been made to extending the theory of computational homogenization to nonlinear regime [20-23] and to improving fidelity and computational efficiency of numerical simulations [24-34]. The fundamental theory that helps to understand the homogenization concept will be shown in Chapter 4.

Reuss and Voigt Methods

The simplest, but not necessarily the best, bounds of homogenization are the Voigt (1889) and Reuss (1929) bounds. The Voigt upper bound on the effective elastic modulus, M_v, of a mixture of N material phases is

$$M_v = \sum_{i=1}^{N} f_i M_i \tag{1}$$

where f_i is the volume fraction of the ith constituent and M_i the elastic modulus of the ith constituent. There is no way that nature can put together a mixture of constituents (e.g., a rock) that is elastically stiffer than the simple arithmetic average of the individual constituent moduli given by the Voigt bound. The Voigt bound is sometimes called the iso-strain average, because it gives the ratio of average stress to average strain when all constituents are assumed to have the same strain.

The Reuss lower bound of the effective elastic modulus, M_R, is

$$\frac{1}{M_R} = \sum_{i=1}^{N} \frac{f_i}{M_i} \tag{2}$$

There is no way that nature can put together a mixture of constituents that is elastically softer than this harmonic average of moduli given by the Reuss bound. The

Reuss bound is sometimes called the iso-stress average, because it gives the ratio of average stress to average strain when all constituents are assumed to have the same stress. Mathematically the M in the Voigt and Reuss formulas can represent any modulus, the bulk modulus K, the shear modulus μ, Young's modulus E, etc.

The simplest example is the elastic behavior of aligned long fiber composites as shown in Figure 2-1.

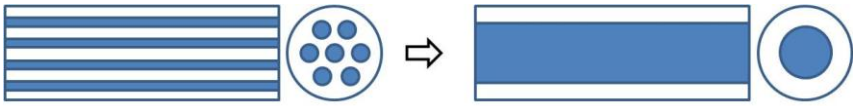

Figure 2-1. Simple uniaxial long fiber composites.

The simplest way to homogenize the elastic behavior is to consider it as a parallel slabs bonded together. Both constituents are under the same strain and this condition is valid for loading along the fiber axis.

$$\varepsilon_1 = \varepsilon_{1f} = \frac{\sigma_{1f}}{E_f} = \varepsilon_{1m} = \frac{\sigma_{1m}}{E_m} \tag{3}$$

For composites having $E_f \gg E_m$, the reinforcement is subject to much higher stress than the matrix and there is a redistribution of the load. The overall stress σ_1 can be expressed in terms of the two contributions. Here f represents the volume fraction of fiber.

$$\sigma_1 = (1-f)\sigma_{1m} + f\sigma_{1f} \tag{4}$$

The elastic modulus of the composites can be written

$$E_1 = \frac{\sigma_1}{\varepsilon_1} = \frac{[(1-f)\sigma_{1m} + f\sigma_{1f}]}{(\frac{\sigma_{1f}}{E_f})} = E_f[\frac{(1-f)\sigma_{1m}}{\sigma_{1f}} + f] \quad (5)$$

This can be simplified using equation (3).

$$E_1 = (1-f)E_m + fE_f \quad (6)$$

This famous Rule of Mixture shows that the global stiffness is simply a weighted average between moduli of the two constituents, depending only on the volume fraction of fibers. The equal strain model is often called as Voigt model, while the method that uses an equal-stress condition is called Reuss model [35].

Ruess model's approach is that the stress acting on the fiber is equal to the stress acting on the matrix when the transverse loading is applied. It is shown in equation (7).

$$\sigma_2 = \sigma_{2f} = \varepsilon_{2f}E_f = \sigma_{2m} = \varepsilon_{2m}E_m \quad (7)$$

Next, the net strain is the sum of the contributions from the matrix and the fiber as

$$\varepsilon_2 = f\varepsilon_{2f} + (1-f)\varepsilon_{2m} \quad (8)$$

Then, elastic modulus of the composites can be written as equation (9) from equation (7) and (8).

$$E_2 = \frac{\sigma_2}{\varepsilon_2} = \frac{\sigma_{2f}}{f\varepsilon_{2f} + (1-f)\varepsilon_{2m}} = \left(\frac{f}{E_f} + \frac{(1-f)}{E_m}\right)^{-1} \quad (9)$$

It is also called inverse rule of mixture.

Eshelby Method

Eshelby's method can be summarized by representing the original inclusion (i.e. fibers) with one made of the matrix material. This is called the equivalent homogeneous

inclusion [9]. This equivalent inclusion is assumed to have an appropriate strain, called the equivalent transformation strain such that the stress field is same with the actual inclusion. The following is a summary of the steps followed in the homogenization procedure according to the Eshelby method which is shown in Figure 2-2.

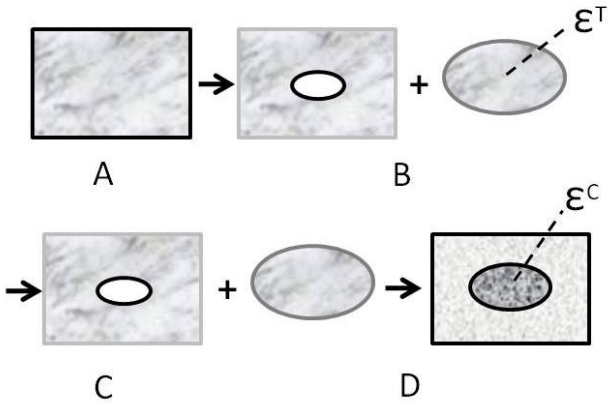

Figure 2-2. Schematic illustration of homogenization by Eshelby method.

Consider an initially unstressed elastic homogeneous material. Imagine cutting an ellipsoidal region (i.e. inclusion) from this material. Imagine also that the inclusion undergoes a shape change free from the constraining matrix by subjecting it to a transformation strain ε^T (B). Since the inclusion has now changed in shape, it cannot be replaced directly into the hole in the matrix material. Imagine applying surface tractions to the inclusion to return to its original shape, then, imagine returning it back to the matrix material (C). Imagine welding the inclusion and matrix material together then removing the surface tractions. The matrix and inclusion will then reach an equilibrium state when the inclusion has a constraining strain ε^C relative to the initial shape before it was removed (D). The stress in the inclusion σ^I can now be calculated as follows assuming the strain is uniform within the inclusion:

$$\sigma^I = C^M(\varepsilon^C - \varepsilon^T) \tag{10}$$

where C^M are the components of the elasticity tensor of the matrix material.

Eshelby has shown that the constraining strain ε^C can be described in terms of the transformation strain ε^T using the equations:

$$\varepsilon^C = S\,\varepsilon^T \tag{11}$$

The Eshelby tensor, S, is a fourth-rank tensor determined using Poisson's ratio of the inclusion material and the inclusion's aspect ratio. This Eshelby tensor or the concept of the Eshelby tensor is widely being used in studies on heterogeneous materials [36]. Finally, the stress in the inclusion is determined by substituting equation (11) into equation (10) and simplifying to obtain:

$$\sigma^I = C^M(S - I)\varepsilon^T \tag{12}$$

where I is the components of the fourth-rank identity tensor. The above equation can be rewritten in matrix forms as follows:

$$\{\sigma^I\} = [C^M]([S] - [I])\{\varepsilon^T\} \tag{13}$$

The braces are used to indicate a vector, while the brackets are used to indicate a matrix. Next, the expressions of the Eshelby tensor, S, are presented for the case of long infinite cylindrical fibers. In this case, the values of the Eshelby tensor depend on Poisson's ratio ν of the fibers and are determined as follows:

$$S_{1111} = S_{2222} = \frac{5 - \nu}{8(1 - \nu)}$$

$$S_{3333} = 0 \tag{14}$$

$$S_{1122} = S_{2211} = \frac{-1 + 4\nu}{8(1 - \nu)}$$

The Eshelby's solution is based on the assumption that the inclusion is in the unbounded, which is infinite, space. This also means that that this is based on the assumption that the constituents are not influenced by each other. So, this method is only applicable to very low volume fraction of heterogeneous materials [37]; i.e., the inclusion is very small compared to the size of matrix and the location of inclusion would not make any difference.

In addition to Eshelby's method of determining the stresses and strains in the fibers and matrix, there are other methods based on Hill's stress and strain concentration factors and self consistent theory [38].

Mori-Tanaka Method

The main difference between Mori-Tanaka and Voigt methods comes from the assumption on the Poisson ratio. The former assumes that the Poisson't ratios of fiber and matrix are different, while the latter assumes they are the same. Mori-Tanaka method is almost same as Eshelby method, but slightly different in taking account of effective strain. Mori-Tanaka method also uses Eshelby tensor. Thus, this method also cannot consider the size and position of fiber.

However, Mori-Tanaka method can be applied to higher concentration of fiber while Eshelby method only can be applied to dilute concentration ($V_f << 1$). In addition to that, when the inclusions is considered as rigid particles, voids ($V_f=0$) and matrix ($V_f=1$), Mori-Tanaka method works better than Eshelby method in those limit case.

Representative Volume Element (RVE)

In most micromechanical analysis of fiber reinforced composite materials, representative unit cell or representative volume element, RVE, is the first step into the analysis. The reason why RVE concept is widely used is the periodic characteristics of fiber composites [39]. In addition to that, unit cell approach can save computational cost for the study on heterogeneous materials. Based on this advantage, it can be applied to characterizing heterogeneous materials with macroscopically and statistically homogeneous structure [40, 41].

For the shape of the RVE, square packing and hexagonal packing are most popular in RVE application for unidirectional fiber composites [42-49]. Several shapes of the unit cell that is possible for the unidirectional fiber composites as shown in Figure 2-4 [50].

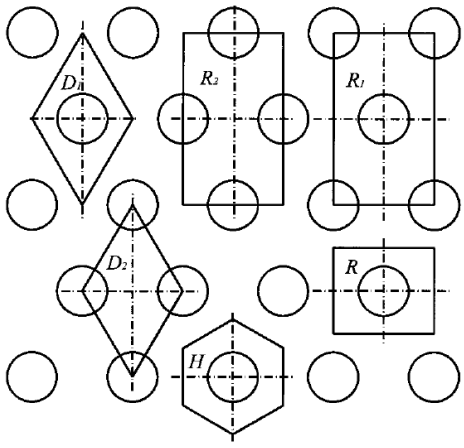

Figure 2-3. Different periodical elements for hexagonal packing.

To be verified as an appropriate RVE, the volume to calculate average composites' behavior need to meet two criteria [51]. First, it must be small enough with respect to the dimensions of the macro scale so that it can be considered as a material

point in the equivalent homogeneous continuum. Second, it must be large enough respect to the scale of the inclusion phase to have elastic properties independent of the loading condition [52]. Although the RVE concept is popular in micromechanical analysis, it seems that the effort to find a proper boundary condition was not given much in researches compared to its popularity. It is not difficult to find a research that only considered the displacement boundary condition for composite analysis [53-55]. To represent the behavior of RVE properly, it is known that not only displacement boundary condition but also traction boundary condition should be applied so that periodicity condition can be satisfied [56]. For this reason, the mixed periodic boundary condition has been the acceptable boundary condition for RVE research [57].

Homogenization for Inelastic Behavior

Research on homogenization or effective properties for nonlinear behavior is still in progress. Most research in this field still considers isotropic hardening and even isotropic behavior [58-60]. It can be easily found that most of inelastic modeling is based on the classical plasticity theory [61-63]. However, it is obvious that the material responses are anisotropic due to the prescribed direction of fiber.

Griffin and Kamat [64] used Hill's orthotropic yield criteria and flow theory along with unidirectional Ramberg-Osgood plastic material model. Similar to the fiber composites, the homogenized materials were modeled as orthotropic elastoplastic one. Although the material behavior in the principal directions is well described by Ramberg Osgood relation [65], the isotropic plasticity equivalent (IPE) material concepts applied was not well matched to the plastic behavior of composite material, which is the focus on the proposed research. Other researches make use of multiaxial Ramberg-Osgood

model for anisotropic material to describe the local inelastic behavior [66, 67]. However, those models are introduced for anisotropic homogeneous materials.

Uncertainty Analysis

To utilize statistical approach, sufficient number of samples within the distribution of the input variables should be prepared. One of the most popular methods to generate random samples is Monte Carlo Simulation (MCS). It is a numerical method based on random sampling and statistical estimation [68]. MCS has been applied to various engineering application of composites; e.g., fatigue and failure modeling [69] and modeling of random properties [70]. Although it is widely used, the classical methods for uncertainty analysis such as standard MCS require a large number of samples in order to estimate the distribution of model output accurately [71]. This is not appropriate for computationally expensive models because it takes too much time to repeat all the samples created by MCS. There have been several approaches to reduce the number of samples for MCS [72]. However these approaches require special knowledge on the response. Because of this, other RSM methods based on series approximation have been developed to reduce the required sample numbers. One of the methods is Stochastic Response Surface Method (SRSM) [73, 74], which is a customized response surface technique for random inputs. A schematic of the steps involved in the uncertainty analysis methods using MCS and SRSM is compared in Figure 2-4 [75].

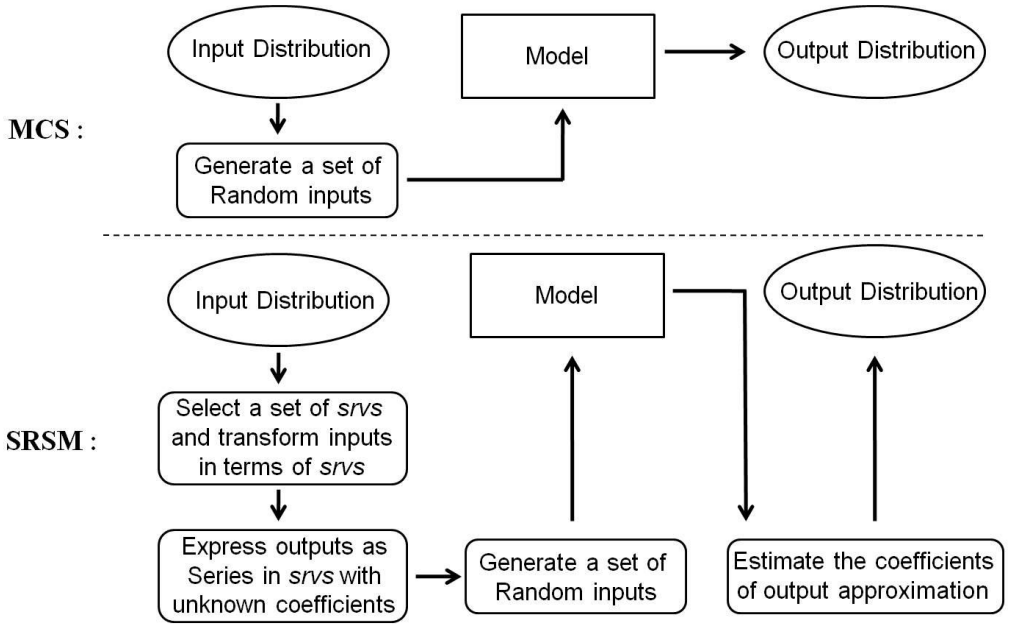

Figure 2-4. Schematic of steps involved in MCS and SRSM.

Another method to overcome the disadvantage of MCS is Latin Hypercube Sampling (LHS). LHS samples based on equally probable intervals while MCS samples randomly. The less independence of LHS on sampling number is the advantage over MCS. There are other types of uncertainty analysis methods, which are based on perturbation techniques [76, 77]. Perturbation based method is effective for a linear problem or a small variation of a stochastic variable but it may not effective for a nonlinear problem or a large variation of variables [78, 79]. A variational method for the derivation of lower and upper bounds for the effective elastic moduli has been studied [80]. There have been several studies on uncertainty of elastic mechanical property. The influence of uncertainty in microscopic properties on homogenized elastic property using the perturbation based analysis [81-83] and polynomial chaos expansion was used for prediction of complex physical system that has several subsystems [84]. Application of uncertainty analysis on elastic behavior can be easily found for aerospace

application. It has complex phenomena and the uncertainty propagation into aerothermoelastic or aeroelastic behavior has been studied [85-87]. Microstructure effect on effective constitutive property was studied using statistical volume element [88] but it does not consider the anisotropic properties.

The study on the uncertainty propagation in multiaxial nonlinear materials behavior is very difficult to find. Some has been done in one dimensional linear hardening or isotropic materials [89-91] but it is not easy to find one associated with anisotropic composite materials.

CHAPTER 3
MATERIAL MODEL

Introduction

Design goals of fiber reinforced composites include high specific strength or stiffness on weight bases. Low density fiber and matrix materials enable high specific strength and moduli composites. The overall mechanical property of composites depends not only on the properties of constituents, but also on the interfacial characteristics. It also depends on the geometrical characteristics of fiber itself. For example, it depends on if fiber is continuous or discontinuous, and if fibers are aligned or randomly oriented, and fibers' shape. There are too many things to consider every aspects of the composites. In this research, for a clear understanding of the validity on approach and result for homogenization and uncertainty analysis, the parameters to be considered are narrowed down to simple but most critical parameters. The bonding region is not considered in modeling. It is one of the most important aspects in composite materials but its effect is too wide to keep track of it. It is important but too much is unknown to be used in homogenization or uncertainty analysis in this research. Thus, material models for fiber and matrix are the only constituents considered in this research for heterogeneous materials.

Fiber Phase

Because of strong bonding in elements of low atomic number, such as C, B, Al and Si, they can form stiff and low density materials. These materials can be made from the elements themselves or from their compounds or oxides such as Al_2O_3 and SiO_2, which can be made to ceramic fibers. The key point is that the flaw exists in these materials, especially the one open to surface, leading to fracture failure. Thus, only the

form of fiber with small radius can enables very high strength applications, and this feature is advantage of fiber reinforcement. It is widely known that the smaller the fiber diameter and the shorter the length, the higher strength, but the greater variability described by Weibulll statistics [92]. Glass fibers are most famous composite materials because of relatively high strength at low cost [93]. High strength glass fibers have been used in structural applications such as pressure vessel since the 1960s that does not require specific stiffness. The other two most popular types are carbon and aramid fibers, while polymer is usually an epoxy, vinylester or polyester thermosetting plastic. Carbon fibers are widely used for aerospace applications but the drawback of the mechanical properties of carbon fibers is its low ductility compared to glass, SiO_2 and Kevlar fibers applications [94]. Table 3-1[95] shows the several fiber materials generally used.

Matrix Phase

The matrix phase for fiber reinforced composites can be a metal, polymer or ceramic. Generally, matrix works as binding materials that supports and protects the fibers and metals and polymers are used because of ductility. As a supporting medium, externally applied stress is transmitted and distributed to the fibers and only a small portion is loaded in matrix phase. It also transfers loading when the fiber is broken. For protection roles, matrix protects fibers from surface damage by chemical reaction or impacts, which can induce surface cracks inducing fracture. Table 3-2 [93] shows properties of some matrix materials.

Table 3-1. Characteristics of several fiber reinforced materials

Material	Specific Gravity	Tensile Strength (GPa)	Specific Strength (GPa)	Modulus of Elasticity (GPa)	Specific Modulus (GPa)
Whiskers					
Graphite	2.2	20.0	9.1	700	318
Silicon nitride	3.2	5.0-7.0	1.6-2.2	350-380	109-118
Aluminum oxide	4.0	10.0-20.0	2.5-5.0	700-1500	175-375
Silicon carbide	3.2	20.0	6.3	480	150
Fibers					
Aluminum oxide	3.9	1.4	0.4	379	96
Aramid (Kevlar 49)	1.4	3.6-4.1	2.5-2.9	131	91
Carbon	1. 8-2.2	1.5-4.8	0.7-2.7	228-724	106-407
E-glass	2.6	3.5	1.3	72	28
Boron	2.6	3.6	11.4	400	156
Silicon carbide	3.0	3.9	1.3	400	133
UHMWPE (Spectra900)	1.0	2.6	2.7	117	121
Metallic Wires					
High strength steel	7.9	2.4	0.3	210	26
Molybdenum	10.2	2.2	0.2	324	31
Tungsten	19.3	2.9	0.2	407	21

Table 3-2. Typical matrix property

Material	Density(Kg/m^3)	Et (GPa)	σ_t (MPa)	ν	α ($10^{-6}/$℃)
Polyester	1200-1400	2.5-4.0	45-90	0.37-0.40	100-200
Epoxy	1100-1350	3.0-5.5	40-100	0.38-0.40	45-65
PVC	1400	2.8	58	…	50
Nylon	1140	2.8	70	…	100
Polyethylene	960	1.2	32	…	120

Epoxy, which is widely used as a matrix material, is a thermosetting polymer [96] and has wide range of applications including fiber reinforced composites and general purpose adhesives. Thermosetting is one of the subdivisions of polymer classification according to the behavior when temperature rises. Thermoplasts are the other division. Thermosetting polymers become permanently hard when heat is applied and do not soften when heat is applied subsequently [95]. Thermosets are basically brittle materials,

while thermoplastics can undergo more plastic deformation. In the same thermosets category, epoxy is tougher and more expensive than vinyl esters, has better resistance to moisture and heat distortion, and shrinks less than polyesters when curing [97]. Because of its better mechanical property, it has been extensively used for aerospace applications.

Elastic Material Model for Fiber

Major type of commercial carbon fiber has tensile modulus in range from 150GPa to 380GPa [98] and most of them have linear elastic behavior as shown in Figure 3-1 [99].

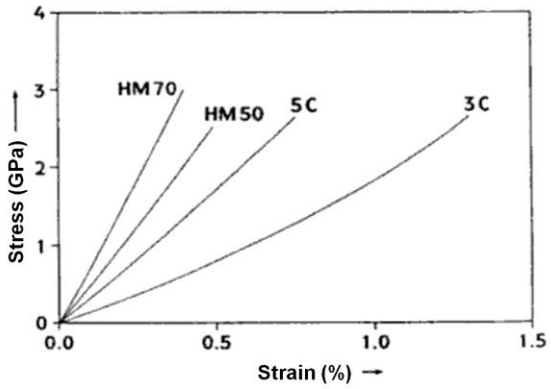

Figure 3-1. Tensile stress-strain curves of pitch-based carbon fibers (HM50, HM70) and PAN-based (3C, 5C).

Therefore, the fiber is assumed to behave linear in this research, and the Young's modulus for fiber is chosen as 224GPa and Poisson ratio of 0.3 based on the data in published literatures. A linear elastic material model is valid for small elastic strains, normally less than 5% [100] and experimental data in Figure 3-1 shows that the strain range that fiber is in application stays less than 5%. Therefore, it is reasonable to assume fiber is linear elastic material.

A linear elastic material's behavior can be defined from the relation of the total stress and total elastic strain as

$$\boldsymbol{\sigma} = \boldsymbol{D}^{el}\,\boldsymbol{\varepsilon}^{el} \tag{1}$$

The $\boldsymbol{\sigma}$ represents the total true stress tensor, $\boldsymbol{D}^{el}$ is the fourth order elasticity tensor, and $\boldsymbol{\varepsilon}^{el}$is the total elastic strain tensor. The simplest form of elasticity is isotropic material, which is considered as the material for fiber in this research and its stress-strain relation is given matrix form in equation (2).

$$\begin{Bmatrix} \varepsilon_{11} \\ \varepsilon_{22} \\ \varepsilon_{33} \\ \gamma_{12} \\ \gamma_{13} \\ \gamma_{23} \end{Bmatrix} = \begin{bmatrix} \frac{1}{E} & -\frac{\nu}{E} & -\frac{\nu}{E} & 0 & 0 & 0 \\ -\frac{\nu}{E} & \frac{1}{E} & -\frac{\nu}{E} & 0 & 0 & 0 \\ -\frac{\nu}{E} & -\frac{\nu}{E} & \frac{1}{E} & \frac{1}{G} & 0 & 0 \\ 0 & 0 & 0 & 0 & \frac{1}{G} & 0 \\ 0 & 0 & 0 & 0 & 0 & \frac{1}{G} \\ 0 & 0 & 0 & & & \end{bmatrix} \begin{Bmatrix} \sigma_{11} \\ \sigma_{22} \\ \sigma_{33} \\ \tau_{12} \\ \tau_{13} \\ \tau_{23} \end{Bmatrix} \tag{2}$$

In equation (2), E is Young's modulus and ν is the Poisson's ratio, G is the shear modulus. The shear modulus also can be expressed in terms of Young's modulus and Poisson's ratio. These input parameters are a function of temperature but the temperature effect is not considered in this research. One thing to be cautious is that Abaqus use engineering strain for shear strain. However, the unidirectional fiber composites is an orthotropic material and the elastic compliance is defined as

$$\begin{Bmatrix} \varepsilon_{11} \\ \varepsilon_{22} \\ \varepsilon_{33} \\ \gamma_{12} \\ \gamma_{13} \\ \gamma_{23} \end{Bmatrix} = \begin{bmatrix} \frac{1}{E_{11}} & -\frac{\nu_{21}}{E_{22}} & -\frac{\nu_{31}}{E_{33}} & 0 & 0 & 0 \\ -\frac{\nu_{12}}{E_{11}} & \frac{1}{E_{22}} & -\frac{\nu_{32}}{E_{33}} & 0 & 0 & 0 \\ -\frac{\nu_{13}}{E_{11}} & -\frac{\nu_{23}}{E_{22}} & \frac{1}{E_{33}} & 0 & 0 & 0 \\ 0 & 0 & 0 & \frac{1}{G_{13}} & 0 & 0 \\ 0 & 0 & 0 & 0 & \frac{1}{G_{23}} & 0 \\ 0 & 0 & 0 & 0 & 0 & \frac{1}{G_{23}} \end{bmatrix} \begin{Bmatrix} \sigma_{11} \\ \sigma_{22} \\ \sigma_{33} \\ \tau_{12} \\ \tau_{13} \\ \tau_{23} \end{Bmatrix} \quad (3)$$

The physical interpretation of $\nu_{ij}$is that it is the transverse strain in the j-direction when the i-direction's stress is applied. It needs to be noted that ν_{ij} is generally not same as ν_{ji}. When $E_{11} = E_{22}$, $\nu_{31} = \nu_{32}$, $\nu_{13} = \nu_{23}$ and $G_{13} = G_{13}$, then it is called transversely isotropic material, which is a subclass of orthotropic material. The RVE used in this research is orthotropic material although the form of stiffness matrix seems alike transversely isotropic because 12-plane that is perpendicular to 3 direction is not actually an isotropic plane that has no directionality on that plane.

Elastoplastic Material Model for Matrix

Matrix is generally made of polymer especially in aircraft applications. Although the characteristic of the polymer is viscoelastic or viscoplastic behavior affected by time, temperature and moisture, the isotropic homogeneous elastoplastic material behavior is considered in this research for the simplicity. Figure 3-2 [101] shows a stress-strain curve for an epoxy material at different temperature. Although the temperature effect is not considered in this research, the matrix behavior is based on the data at 25^{o}C.

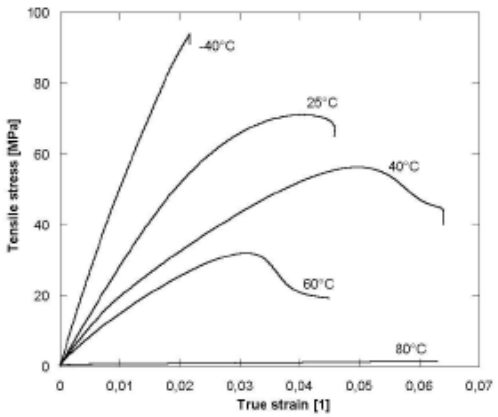

Figure 3-2. Stress-strain curves of epoxy L135i measured at different temperatures.

Based on these data, the elastoplastic material behavior is implemented into Abaqus finite element (FE) analysis. The schematic drawing of the constitutive behavior of these two material models are shown in Figure 3-3.

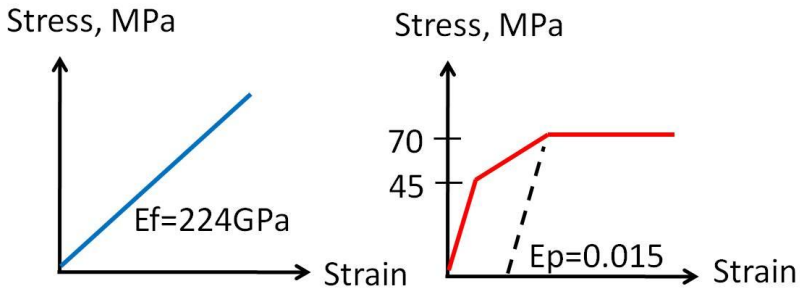

Figure 3-3. Elastic material for fiber and elastoplastic material for matrix.

The elastoplastic material is modeled with two yield point. One is for the end point of linear elastic region, which is 45MPa and the other is at 75MPa that begins perfect plastic deformation. The plastic strain when the perfect plastic region begins is given as 0.015 based on the stress-strain curve in Figure 3-2.

For the plasticity model implemented in the library in Abaqus FE program, it approximates the smooth stress-strain behavior of the material with piecewise linear

curves joining the given data points. Any number of points can be used to approximate the actual material behavior, which means it can be used as a very close approximation of the actual material behavior as shown Figure 3-4.

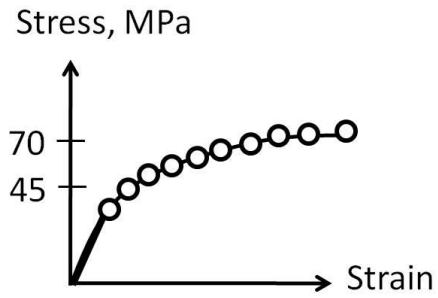

Figure 3-4. Example of data input for material model in Abaqus.

When the stress-strain relation is given by strain dependent properties instead of constants, it behaves nonlinearly. Computational challenges come from the fact that the equilibrium equations should be written using material properties that depends on the strains, which are not known in advance. In order to describe the plastic stresses-strains relation, conventional plasticity theory uses yield criterion that define the condition of the onset of inelastic behavior. This yield condition is generally defined by a yield function $f = (\sigma, R)$ described by stress, σ, and hardening equivalent stress, R. When R=0, yield occurs when equivalent stress value reaches the initial yield stress, σ_y.

This hardening stress can be a constant for linear strain hardening or a function of plastic strain for isotropic hardening and a function of both stress and strain for kinematic hardening. So, the yield occurs when the equation (4) is satisfied.

$$f(\sigma, R) = \sigma_{eq} - \sigma_y - R = 0 \tag{4}$$

Equation (4) is called yield surface and it is worth to note that is a scalar equation.

The material is in elastic region when f < 0 and in inelastic region otherwise. However, f > 0 cannot be occur physically and f = 0 whenever it is in elastic region. It is called consistency condition. Since the stress must be on the yield surface and the size of the yield surface is related to the magnitude of the accumulated plastic strain, the magnitude of the plastic strain increment also must be related to the stress increment. This relation produced plastic flow rule defined as equation (5) [102].

$$\dot{\varepsilon}_{ij}^{p} = \dot{\lambda} N_{ij}, \;\; N_{ij} = \frac{\partial f}{\partial \sigma_{ij}} \tag{5}$$

These yield function and flow rule are the fundamental of classical plasticity theory.

Different yield criteria have their own definition for the terms used in equation (4). For example, isotropic von Mises yield criteria [103] the equivalent stress is defined as equation (6) and S_{ij} denotes deviatoric stress.

$$\sigma_{eq} = \sqrt{\frac{3}{2} S_{ij} S_{ij}}, \qquad S_{ij} = \sigma_{ij} - \frac{1}{3} \sigma_{mm} \delta_{ij} \tag{6}$$

Beyond yield point, stresses are related to strains by incremental constitutive relation. When the Hook's law and the relation between total strain, elastic strain and plastic strain, the constitutive relation becomes as

$$\dot{\sigma}_{ij} = C_{ijkl} \, \dot{\varepsilon}_{kl}^{e} = C_{ijkl} (\dot{\varepsilon}_{ij} - \dot{\varepsilon}_{kl}^{p}) = C_{ijkl}^{ep} \dot{\varepsilon}_{kl} \tag{7}$$

where C_{ijkl}^{ep} is the elastoplastic tangent operator that relate the stress and total strain. From equation (5) and (7), we can see that tangent operator is a function of $\dot{\lambda}$ which is called plastic consistency parameter or plastic multiplier.

Since the yield surface should be updated whenever the loading is applied beyond yield point, the yield surface also should be updated using accumulated plastic strain at that point. The updated yield function can be written as

$$f^{n+1} = f^n + df = 0 \tag{8}$$

Without expanding the equation (8) in detail, we can see that it is a nonlinear equation in terms of $\dot{\lambda}$. This equation can be solved to compute $\dot{\lambda}$ using the local Newton-Raphson method. If isotropic/kinematic hardening is a linear function of $\dot{\lambda}$, or the effective plastic strain, then only one iteration is required to calculate the every components updated points. After $\dot{\lambda}$ is found, stress, effective strain and hardening parameters can be obtained.

As has been shown above, the material constituent of elastoplastic material can be calculated algorithmically. Equation (7) relates infinitesimal stress increments with corresponding infinitesimal strain increment at a given state. However, the iteration for equilibrium is carried out in a finite magnitude rather than infinitesimal one. Therefore, Abaqus carries out the global iteration to find structural equilibrium, while the user subroutine (UMAT) that models material behavior requires local iteration to calculate the incremental constitutive model. These are the core of elastoplastic materials FE analysis and also are the main reasons it cost a lot of time especially when it has more than two materials.

Another issue when approached using conventional plasticity theory represented by equation (4) is that the yield point is decided by equivalent stress which is a scalar, even if three dimensional stress and strain components are involved. To compensate for this issue when it is applied to anisotropic materials, Hill introduced anisotropic yield

criteria [104] and modified versions have introduced since then [105-107]. Hill's or its modified versions of anisotropy yield criteria are to define anisotropic yield point, which means that the direction dependency is considered. However these yielding criteria have nothing to do with hardening, which describe the behavior of material after yielding. Consequently, anisotropic hardening should be considered, which is not easy as long as equivalent stress is used. The homogenization model in this research can reduce the local iterations by applying tensor form of Ramberg-Osgood model and application of anisotropy tensor solves the anisotropy issues.

Ramberg and Osgood introduced simple formula to describe stress-strain curve in terms of three parameters in 1943 [108] as equation (9).

$$e = \frac{S}{E} + K\left(\frac{S}{E}\right)^{n} \tag{9}$$

where s is stress, e is strain and K and n are constants.

In contrast to the classical plasticity model, Ramberg-Osgood model describe entire materials behavior in an equation without defining any yield point and it is adequate to represent stress-strain curve that does not have sharp yield point. It was originally introduced for uniaxial loading condition and the modified form for the multiaxial loading condition is used in this research. More details of multiaxial Ramberg-Osgood model are discussed in Chapter 4.

CHAPTER 4
HOMOGENIZATION USING RVE

Introduction

In a small scale, all materials are heterogeneous. To understand and be convinced of all the mechanism at a high degree of accuracy, one should investigate all phenomena that occur at atomic or molecular scale. When engineering materials were to be designed at this level of accuracy, the required amount of computational resources would be out of practicality. Figure 4-1 shows that only a portion of the unidirectional fiber composites, and its analysis to calculate stress and strain components under uniaxial static tension loading took more than 20 hours based on 64bit Pentium 3.4GHz processor.

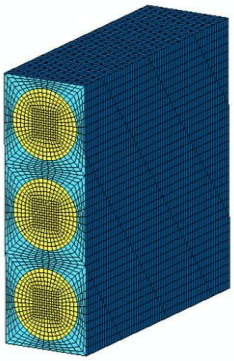

Figure 4-1. Unidirectional fiber composites composed of nine RVEs.

In this chapter, homogenization of composite material for elastic behavior is performed on a representative volume element, RVE. For a brief comparison, it took 17 minutes for a simple tension loading. Heterogeneous materials can be geometrically represented by the concept of periodicity as shown in Figure 4-2 and the uniaxial fiber

composites can be regarded as the periodic materials composed of blocks of representative volume element, RVE.

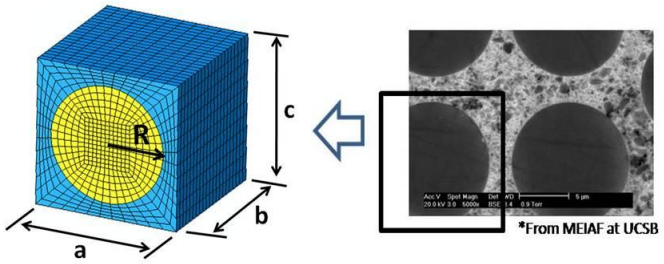

Figure 4-2. RVE used in this research for uniaxial fiber composites.

Performing an analysis on the RVE, not on entire engineering structure, one can reduce the computational time to understand the mechanical behavior of composite material. But, it requires appropriate boundary condition so that the RVE can be analyzed as a component in the middle of the structure, not as an independent, separate one. This is why the boundary condition for the RVE is important. The different results from different boundary condition are shown later. In this research, the periodic boundary condition contains both periodic displacement boundary condition and periodic traction boundary condition, which also called as mixed periodic boundary condition. The important issues on this periodic boundary condition are also discussed later. A different approach from the RVE concept used for elastic application will be applied for the homogenization for inelastic behavior. However, when the simulation of entire structure is required, not micro mechanical study, even this heterogeneous RVE cannot give any cost saving because it has to be assembled again to compose entire structure as heterogeneous. So, heterogeneous RVE can save cost for the micro scale

analysis alone but not for the macro scale analysis or simulation such as manufacturing process.

One of the hypotheses to overcome this difficulty that arises for larger scale analysis is that the structure of the material is considered as a continuum. This means that there exist measures associated with properties that govern the behavior of the media, and the properties of material at a point can be computed using an averaging scheme. These properties are actually similar to the averages of very complicated interactions and phenomena in the atomic scale. Likewise, homogenization is similar to the continuum concept in terms of the homogenized medium that has properties governing the behavior of the heterogeneous media. In this research, the mean field theory is applied, which is also known as the average field theory. Using this theory, macro field is defined as the volume average of corresponding micro fields. This average scheme was introduced for analytical methods in earlier researches; i.e., Reuss and Voigt method as discussed in the Chapter 2. The main issue of the analytical method is that it is valid only under a specific condition. For example, whenever the shape or the position of fiber changes, the analytical expression for averaged properties should be derived again. Furthermore, it is very difficult to formulate all complex geometry effects and nonlinear behaviors. On the contrary, numerical method does not have these limitations. As the computational power continues to grow as technology advances, it enables calculation of more complicated geometry and reduces the number of assumptions in the model. For this reason, the numerical method is used in this research using a commercial program, Abaqus. Python script is written in order to calculate effective properties as a post process from numerical model and to generate

parameterized heterogeneous RVEs. As the Abaqus has strength in capability of user customized material, anisotropic hardening Ramberg-Osgood model was implemented using a FORTAN code for the user subroutine (UMAT).

At this point, it needs to be mentioned that the RVE approach gives approximate macro scale understanding of the composites because there is no exact periodicity in real random media. It could get closer to the more accurate analysis results when the real composites has higher periodicity.

Representative Volume Element (RVE)

The heterogeneous RVE used in this research has been built using a commercial FE program, Abaqus. In this research, three-dimension square unit cell is considered as a RVE because it is relatively easy to impose symmetry and periodic boundary conditions compared to the hexagonal one as discussed in Chapter 2 briefly.

RVE is a unit size cube having dimensions of a=1, b=1 and c=1 as shown in Figure 4-2. A total of 11781 C3D8 elements are used to model the RVE. The stress and strains are calculated at the eight integration points in each element, and the output data from entire RVE are post processed to calculate required values for statistical analysis using Python and Matlab. The RVE part has mapped mesh on every outer surface so that constraint equations between opposite facing nodes can be constructed. How the constraint equation and periodic boundary condition are applied is discussed later.

The RVE has two materials. One is an isotropic homogeneous uniaxial fiber parallel to z axis and the other is an isotropic homogeneous matrix. The materials for fiber and matrix are described detail in Chapter 3. The radius and the center of the fiber are parameterized as variables for statistical analysis. A perfect bonding between the

fiber and matrix is assumed for simplicity because the delamination or boundary effect is not covered in this research.

Boundary Condition

As the RVE is not distinguishable from the next in the periodic structure, it can be said that the response of the entire composite structure under uniform macroscopic loading is same as the response of the RVE under the same loading condition. To apply the RVE concept to the periodic composite materials, the appropriate periodic boundary condition is an important part of modeling. The Figure 4-3 shows that how the distributions of von Mises stress is different in the heterogeneous RVE according to different boundary conditions on the surface. When the RVE does not have any constraints and can deform freely, the deformed shape has curved shape under normal tension and under shear tension.

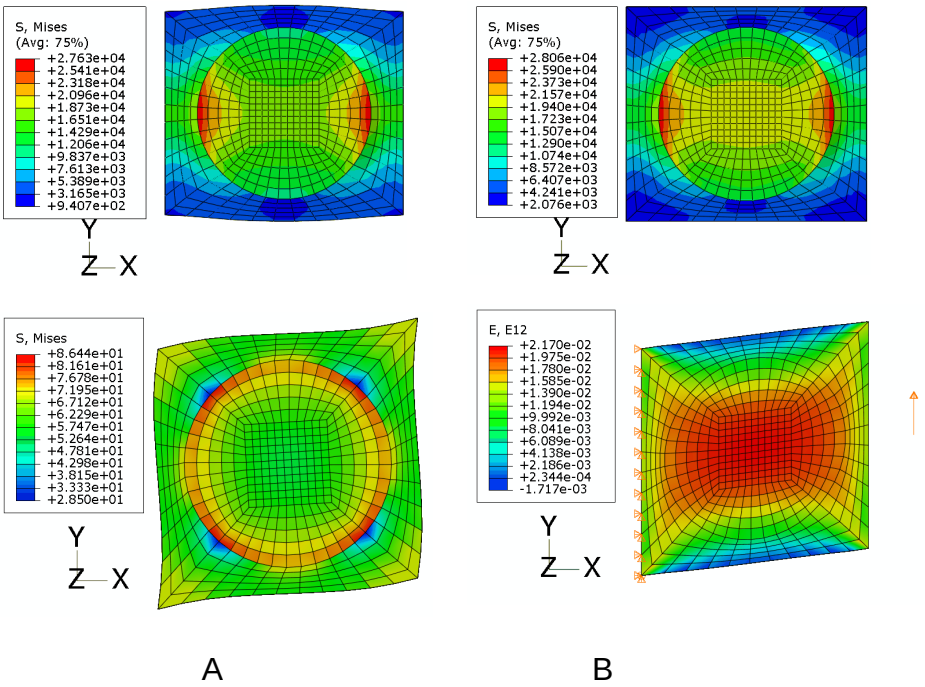

A B

Figure 4-3. von Mises stress. A) not constrained. B) constrained to be flat.

When the boundary of the RVE has constrained not to move in transverse direction, it results in local or overall higher stress. When the shear is applied on the RVE whose transverse direction surface to be flat, it has high stress induced inside.

However, most studies on the effect of the boundary condition were performed for the elastic behavior or elastic mechanical property. In the process of the homogenization study in this research, the effect of boundary condition in inelastic behavior is also discussed. Figure 4-4 shows that the deformed shape of the RVE that is under uniaxial x-direction tension without constraining boundary condition. As both top and bottom surface has a bulged out shape due to hard fiber in center, it cannot compose a periodic structure, and consequently, cannot be used as a representative volume element. Thus, proper boundary condition is required so that the behavior of the RVE can represent entire periodic structure. The RVE requires constraints that related the nodes on the opposite side of RVE so that the opposite sides deform in the same shape, which make the geometric periodic.

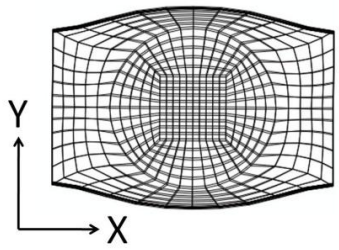

Figure 4-4. Volume element deformed without periodic boundary condition.

Periodic Boundary Condition

First, it would be better to know about the displacement boundary condition that sometimes applied to the RVE as a periodic boundary condition, which is not

appropriate. It is when a RVE is subject to displacement field on the boundary in the form:

$$U_i|_s = \bar{\varepsilon}_{ij} d_j \tag{10}$$

The s denotes each boundary surface and $d_j$is the size of the RVE in j direction. When $\bar{\varepsilon}_{ij}$ is a constant strain, the average or effective strain $\bar{\varepsilon}_{ij}$ is same as the applied constant strain, i.e., $\varepsilon_{ij}^0 = \bar{\varepsilon}_{ij}$ assuming fiber and matrix is perfectly bonded. Application of this homogeneous displacement boundary condition to a RVE results in the flat surface remain flat after deformation. This condition is inappropriate because the RVE is heterogeneous and has a fiber that is generally harder than the matrix in the center; the deformation of the surface cannot remain flat after deformation. If boundary surfaces are forced to be flat when it has to deform to have wavy surface, it will be over constrained and the result will be different. On the contrary, the periodic displacement boundary condition constrains the boundary in pair facing opposite each other, i.e. the plane at the coordinate x=0 and the plane at the coordinate x=1 when the dimension of the RVE is unit (d_x=1). The periodic displacement boundary condition constrains the boundary to keep the relative displacement constant according to the strain on that boundary as shown in Figure 4-5.

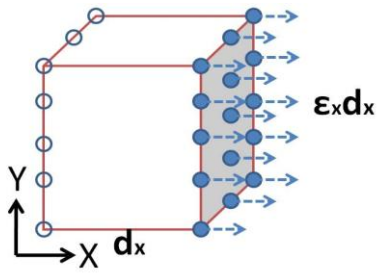

Figure 4-5. Periodic displacement boundary condition in x direction.

The periodic displacement boundary conditions can be assigned considering the deformation of a RVE relative to a fixed global coordinate. The displacement $u(x_0)$ of a point x_0 in an x coordinates in RVE need to be considered first. Then the characteristic distance d that does not dependent on a location of x_0 defines the size of the RVE in x direction. From this concept, the periodic boundary condition can be expressed as follows:

$$u_i(x_0 + d) = u_i(x_0) + \bar{\varepsilon}_{ij} d_j \tag{11}$$

where $\bar{\varepsilon}_{ij}$ is the average strain component. Y and Z direction also has periodic displacement boundary condition same way.

As this boundary condition is only available for the RVE that has opposite face, the periodic boundary condition cannot be applied when the RVE that has triangular shape or when the number of the nodes on the facing planes are different.

Besides to the periodic displacement boundary condition, the traction boundary condition should be satisfied as well. The traction boundary condition can be written as

$$t_i(x_0 + d) = -t_i(x_0) \tag{12}$$

where t denotes traction on the boundary. Y and Z direction also has periodic traction boundary condition same way.

Equation (11) and (12) define the periodic boundary condition that hold for arbitrary microstructure in the RVE. This periodic boundary condition is applied to both elastic and inelastic behavior analysis in this research.

In practical implementation in Abaqus, the periodic boundary conditions are imposed using multi-point constraints (MPC). MPC can impose a relationship between

different degree-of-freedoms in the numerical model. In general, multiple dependent degrees-of-freedom can be related to a single independent degree-of-freedom.

Application of UVE in Structure

The periodic boundary condition is applied to calculating elastic stiffness matrix from the RVE in this research and the detail is presented when homogenization is discussed. The periodic boundary condition is inevitable to calculate effective stiffness matrix when macro-scale strains are applied to the RVE. However, as the periodic boundary condition is not a perfect boundary condition, there have been studies on its effect on homogenized material properties. Drago and Pindera presented the periodic displacement boundary condition as the upper bound of effective properties and the periodic traction boundary condition as the lower bound [57]. One disadvantage of periodic boundary condition is that it is limited to a symmetric shape of the RVE. It is well known that it has unrealistically stiff response on the boundary [109].

Since obtaining accurate effective mechanical properties is the key in homogenization, it is necessary to verify the accuracy of periodic boundary condition first. However, it should be noted that the periodic boundary condition is not a requirement for the homogenization process but for the application of the RVE concept to keep its periodic characteristics. It means that the periodic boundary condition itself has nothing to do with the process of effective property calculation if the properties are available directly from the entire composite structure. For the verification, the behavior of the RVE that has periodic boundary condition and the behavior of a volume region that is called UVE in the heterogeneous structure are compared in Figure 4-6. The UVE is a unit volume, as shown in Figure 4-7, which is geometrically same as RVE, in the

composite structure in which the stress and strain is calculated. The UVE is named to distinguish from the RVE.

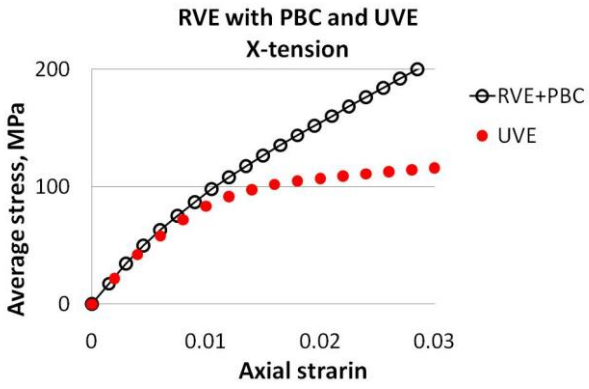

Figure 4-6. X direction stress in the RVE with periodic boundary condition and UVE.

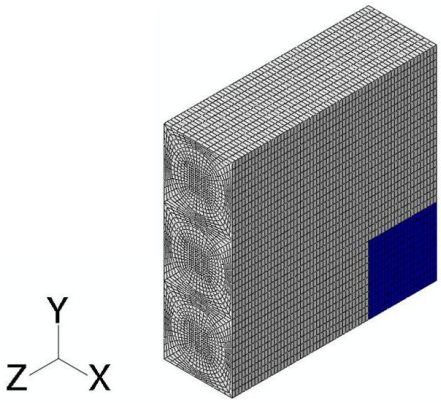

Figure 4-7. The unit volume element UVE in the composite structure.

It shows that the behavior of the RVE and the UVE is almost same in elastic region but not in the plastic region. Based on the assumption that the UVE represent more close to real composites' behavior, the application of the RVE with periodic boundary condition to the elastic analysis is allowable but not in plastic region. Thus, the properties obtained from the RVE are used to homogenize elastic behavior and UVE is

used to inelastic behavior. The size of composite structure that surrounds UVE is discussed later for homogenization for inelastic behavior.

Homogenization for Elastic Behavior

As the fiber is modeled elastic material, RVE will behave elastically when the matrix behaves in elastic region. Elastic behavior of materials can be described by elastic mechanical properties such as elastic Young's modulus, Poisson ratio and so on. Since individual constituents are elastic, the combination of them will also be elastic. These elastic mechanical properties can be narrowed down to the relation between stress and strain, represented by the stiffness matrix. Table 4-1 shows the elastic mechanical properties for the constituents used in the RVE.

Table 4-1. Mechanical property of constituents

Ef	(modulus of fiber)	224GPa
Em	(modulus of matrix)	3.5GPa
νf	(Poisson of fiber)	0.3
νm	(Poisson of matrix)	0.26
Vf	(fiber volume fraction)	50%

The constitutive law for the RVE can be determined based on these mechanical properties and to have effective stiffness that can represent overall or global stiffness. The average scheme is used to calculate the macro stress, which generally defined as volume average in RVE, as [110]

$$\overline{\sigma}_{ij} = \frac{1}{V}\int_{V} \sigma_{ij} dV \tag{13}$$

where $\sigma_{ij}$is the true stresses in the RVE or micro stresses.

As RVE itself is composed of small elements, to perform volume integral, the Gaussian Quadrature Integration method is applied for each element

$$\overline{\sigma}_{\mathrm{ij}} = \frac{1}{\mathrm{V}} \sum_{\mathrm{i=1}}^{\mathrm{NE}} \int_{\mathrm{V}} \sigma_{\mathrm{ij}}\, \mathrm{dV_i} = \frac{1}{V} \sum_{e=1}^{element} \sum_{k=1}^{int} \left(\sigma_{ij}\right)_k V_e \tag{14}$$

To have all the stress values in every meshed element in RVE, a commercial finite element program is used. Each stress component in every meshed element is calculated and then using vector operation command, all the stresses having same index in element are summed up. As there are six stress indices for isotropic material, the resultant effective stress that represents whole RVE stress state will be a 6 by 1 vector. The effective constituents can be expressed as

$$\begin{Bmatrix} \overline{\sigma}_{\mathrm{xx}} \\ \overline{\sigma}_{\mathrm{yy}} \\ \overline{\sigma}_{\mathrm{zz}} \\ \overline{\sigma}_{\mathrm{xy}} \\ \overline{\sigma}_{\mathrm{yz}} \\ \overline{\sigma}_{\mathrm{xz}} \end{Bmatrix}_{\mathrm{eff}} = [\overline{\mathrm{C}}]_{\mathrm{eff}} \begin{Bmatrix} \overline{\varepsilon}_{\mathrm{xx}} \\ \overline{\varepsilon}_{\mathrm{yy}} \\ \overline{\varepsilon}_{\mathrm{zz}} \\ \overline{\varepsilon}_{\mathrm{xy}} \\ \overline{\varepsilon}_{\mathrm{yz}} \\ \overline{\varepsilon}_{\mathrm{xz}} \end{Bmatrix}_{\mathrm{eff}} \tag{15}$$

As the strains are given (in fact, it is applied as a boundary condition) and the stresses in each element are calculated, the components of the stiffness matrix, $[\overline{\mathrm{C}}]_{\mathrm{eff}}$, can be obtained. Using simple algebraic manipulation, the effective stiffness component is obtained using FEM program and averaging scheme. For example, when $\overline{\varepsilon}_{\mathrm{xx}} = 1$ is applied and all other macro-scale strains are zeros, the averaged stresses become the first column of the effective stiffness matrix, i.e.:

$$\begin{Bmatrix} \bar{C}_{11} \\ \bar{C}_{22} \\ \bar{C}_{33} \\ \bar{C}_{12} \\ \bar{C}_{23} \\ \bar{C}_{13} \end{Bmatrix}_{\text{eff}} = \begin{Bmatrix} \bar{\sigma}_{xx} \\ \bar{\sigma}_{yy} \\ \bar{\sigma}_{zz} \\ \bar{\sigma}_{xy} \\ \bar{\sigma}_{yz} \\ \bar{\sigma}_{xz} \end{Bmatrix}_{\text{eff}} \tag{16}$$

As we have effective elastic stiffness matrix, we can obtain effective global stress directly from applied strain using constitutive equation without modeling both fiber and matrix together, which is computationally expensive.

The RVE is an orthotropic material but it can be transversely isotropic materials when the uniaxial fiber is at the center of the RVE. The transversely isotropic materials (five independent constants) stiffness matrix is obtained by Abaqus analysis for RVE.

$$[\bar{C}]_{\text{eff}} = \begin{bmatrix} \bar{C}_{11} & \bar{C}_{12} & \bar{C}_{13} & 0 & 0 & 0 \\ \bar{C}_{12} & \bar{C}_{11} & \bar{C}_{13} & 0 & 0 & 0 \\ \bar{C}_{13} & \bar{C}_{13} & \bar{C}_{33} & 0 & 0 & 0 \\ 0 & 0 & 0 & \bar{C}_{44} & 0 & 0 \\ 0 & 0 & 0 & 0 & \bar{C}_{55} & 0 \\ 0 & 0 & 0 & 0 & 0 & \bar{C}_{55} \end{bmatrix} \tag{17}$$

Furthermore, from following relation between compliance matrix, S, and the elastic property, we can calculate effective elastic properties from the stiffness matrix of the RVE.

$$S = \begin{bmatrix} S_{11} & S_{12} & S_{13} & 0 & 0 & 0 \\ S_{12} & S_{11} & S_{13} & 0 & 0 & 0 \\ S_{13} & S_{13} & S_{33} & 0 & 0 & 0 \\ 0 & 0 & 0 & S_{44} & 0 & 0 \\ 0 & 0 & 0 & 0 & S_{55} & 0 \\ 0 & 0 & 0 & 0 & 0 & S_{55} \end{bmatrix} \tag{18}$$

$$= \begin{bmatrix} \frac{1}{E_{11}} & -\frac{\nu_{21}}{E_{22}} & -\frac{\nu_{31}}{E_{33}} & 0 & 0 & 0 \\ -\frac{\nu_{12}}{E_{11}} & \frac{1}{E_{22}} & -\frac{\nu_{32}}{E_{33}} & 0 & 0 & 0 \\ -\frac{\nu_{13}}{E_{11}} & -\frac{\nu_{23}}{E_{22}} & \frac{1}{E_{33}} & 0 & 0 & 0 \\ 0 & 0 & 0 & \frac{1}{G_{12}} & 0 & 0 \\ 0 & 0 & 0 & 0 & \frac{1}{G_{13}} & 0 \\ 0 & 0 & 0 & 0 & 0 & \frac{1}{G_{23}} \end{bmatrix} \quad (19)$$

The E_{11}, E_{22} and E_{33} are the extensional moduli of elasticity along the 1, 2, and 3 directions, respectively. Also, ν_{ij} (i, j = 1, 2, 3) are the Poisson's ratios, and G_{12}, G_{23}, and G_{13} are the shear moduli. It is clear that there are only five independent material constants ($E_{11}, E_{33}, \nu_{12}, \nu_{31}, G_{32}$) for a transversely isotropic material. $\nu_{13}$is dependent of $E_{11}, E_{33}, \nu_{31}$and can be calculated by

$$\frac{\nu_{31}}{E_{33}} = \frac{\nu_{13}}{E_{11}} \quad (20)$$

A material is called isotropic when its property is the same in all three directions. In that case, $E_{11} = E_{22} = E_{33} = E,\ \nu_{12} = \nu_{31} = \nu_{32} = \nu, and\ G_{12} = G_{31} = G_{32} = G$. There are only two independent material constants (E, ν) for an isotropic material.

However, anisotropic materials have nonzero entries at the upper right and lower left portions of their compliance and stiffness matrices. The components of the compliance matrix have following relation with stiffness matrix components.

$$S_{11} = \frac{(C_{11} * C_{33} - {C_{13}}^2)}{(C_{33} * {C_{11}}^2 - 2C_{11} * {C_{13}}^2 - {C_{12}}^2 * C_{33} + 2C_{12} * {C_{13}}^2)} = \frac{1}{E_{11}} \quad (21)$$

$$S_{12} = -\frac{(C_{12} * C_{33} - {C_{13}}^2)}{(C_{33} * {C_{11}}^2 - 2C_{11} * {C_{13}}^2 - {C_{12}}^2 * C_{33} + 2C_{12} * {C_{13}}^2)} = \frac{-\nu_{21}}{E_{22}} \quad (22)$$

$$S_{13} = -\frac{C_{13}}{(C_{11} * C_{33} - 2{C_{13}}^2 + C_{12} * C_{33})} = \frac{-\nu_{31}}{E_{33}} \quad (23)$$

$$S_{33} = \frac{(C_{11} + C_{12})}{(C_{11} * C_{33} - 2{C_{13}}^2 + C_{12} * C_{33})} = \frac{1}{E_{33}} \quad (24)$$

$$S_{44} = \frac{1}{C_{44}} = \frac{1}{G_{12}} \quad (25)$$

$$S_{55} = \frac{1}{C_{55}} = \frac{1}{G_{13}} \quad (26)$$

Table 4-2 shows the calculated effective elastic mechanical properties calculated by the stiffness matrix components and compliance matrix when the fiber volume fraction is 50% and the material properties in Table 4-1 are used. As expected, the stiffness in the fiber-direction (E_{33}) is an order of magnitude larger than that of other two directions.

Table 4-2. Effective elastic properties

Effective elastic property	Value [GPa]
$\bar{E}_{11} = \bar{E}_{22}$	10.92
$\bar{E}_{33}$	113.90
$\bar{\nu}_{21} = \bar{\nu}_{12}$	0.22
$\bar{\nu}_{31} = \bar{\nu}_{32}$	0.28
$\bar{G}_{12} = \bar{C}_{44}$	2.97
$\bar{G}_{13} = \bar{G}_{23} = \bar{C}_{55}$	4.09

The stiffness matrix obtained from RVE model can be compared to the stiffness matrix obtained from Eshelby method as shown in Table 4-3 and Mori-Tanaka method in Table 4-4. As expected, ‘Mori-Tanaka’ method gives closer results to Abaqus results than ‘Eshelby’ method.

Table 4-3. Effective stiffness matrix from Eshelby method

7.31	2.43	-4.42	0	0	0
2.43	7.31	-4.42	0	0	0
2.69	2.69	110.96	0	0	0
0	0	0	3.44	0	0
0	0	0	0	4	0
0	0	0	0	0	4

Table 4-4. Effective Stiffness matrix from Mori-Tanaka method

10.40	3.62	3.98	0	0	0
3.62	10.40	3.98	0	0	0
3.98	3.98	116.01	0	0	0
0	0	0	3.39	0	0
0	0	0	0	4	0
0	0	0	0	0	4

The Voigt and Reuss method which is known to give upper and lower bounds of the stiffness components are calculated. The results in Tables 4-5 and 4-6 show that the calculated elastic properties are within the bounds. The effective elastic properties are compared in Table 4-5 and Table 4-6 for volume fraction 50%.

In fiber volume fraction of 50%, axial direction estimates, $\bar{E}_{33}$, are close to each other but in transverse direction, $\bar{E}_{11}$, the analytical methods give big discrepancy. The results show that the Ruess' lower bound is poor approximation in transverse direction.

Table 4-5. Young's modulus compared to upper bound (Vf=50%)

	Abaqus RVE	Eshelby	Mori-Tanaka	$v_f E_f + (1 - v_f) E_m$
$\bar{E}_{33}$	113.90	106.95	113.75	114.35
Difference	0%	-6.0%	-0.1%	+0.4%

Table 4-6. Young's modulus compared to lower bound (Vf=50%)

	Abaqus RVE	Eshelby	Mori-Tanaka	$\frac{E_f * E_m}{v_f * E_m + v_m * E_f}$
$\bar{E}_{11}$	10.93	6.42	9.08	6.93
Difference	0%	-41.3%	-16.9%	-36.6%

Effect of the Volume Fraction

The fiber volume fraction is decreased from 50% to 5% and the stiffness matrix and the elastic properties calculated based on the RVE, Eshelby and Mori-Tanaka method are compared. As can be seen in Tables 4-7, 4-8, and 4-9, all three methods yield similar effective elastic properties. This is because for small volume fraction, the interaction between fibers can be negligible.

Table 4-7. Effective Stiffness from ABAQUS (Vf= 5%)

4.62	1.61	1.64	0	0	0
1.61	4.62	1.64	0	0	0
1.64	1.64	15.32	0	0	0
0	0	0	1.49	0	0
0	0	0	0	1.53	0
0	0	0	0	0	1.53

Table 4-8. Effective stiffness from Eshelby method (Vf= 5%)

4.59	1.60	0.91	0	0	0
1.60	4.59	0.91	0	0	0
1.62	1.62	14.95	0	0	0
0	0	0	1.59	0	0
0	0	0	0	1.65	0
0	0	0	0	0	1.65

Table 4-9. Effective Stiffness from Mori-Tanaka method (Vf= 5%)

4.61	1.62	1.64	0	0	0
1.62	4.61	1.64	0	0	0
1.64	1.64	15.39	0	0	0
0	0	0	1.50	0	0
0	0	0	0	1.53	0
0	0	0	0	0	1.53

The lower the fiber volume fraction, the closer the Eshelby method to the Abaqus result. However, the Mori-Tanaka method is always closer than that of the Eshelby method. Axial and transverse direction Young's modulus are compared in Table 4-10

and Table 4-11. Therefore, it can be concluded that for a low fiber volume fraction, analytical methods can predict the effective elastic properties accurately, but the Mori-Tanaka method is closer than that of Eshelby method.

Table 4-10. Young's modulus compared to upper bound (Vf =5%)

	Abaqus RVE	Eshelby	Mori-Tanaka	$v_f E_f + (1 - v_f) E_m$
$\bar{E}_{33}$	14.45	14.47	14.53	14.53
Difference	0%	+0.14%	+0.55%	+0.55%

Table 4-11. Young's modulus compared to lower bound (Vf =5%)

	Abaqus RVE	Eshelby	Mori-Tanaka	$\frac{E_f * E_m}{v_f * E_m + v_m * E_f}$
$\bar{E}_{11}$	3.98	3.99	3.97	3.68
Difference	0%	+0.25%	-0.25%	-7.5%

As expected, the discrepancy in transverse direction Young's modulus, $\bar{E}_{11}$ reduced when fiber volume fraction is reduced compared to Table 4-6. However, the difference of axial direction Young's modulus $\bar{E}_{33}$ for Mori-Tanaka is slightly increased when fiber volume fraction is reduced.

Effect of the Fiber Crack

So far, the effective elastic properties for perfect fiber-matrix composites are considered. However, it is often possible that some of fibers are damaged, and as a result, the effective elastic modulus can significantly different from the perfect one. The effect of the fiber crack on elastic stiffness is investigated in this section. The crack, which is a discontinuity, is modeled as enriched feature. The extended finite element method (XFEM) uses the enriched feature and is an extension of general FEM allowing the discontinuities to exist in an element by enriching degrees of freedom with special displacement functions. This method is efficient especially when the crack propagation is to be investigated as the conventional FEM have to re-mesh and update continuously

through the entire structure. In this research, since the effect of the crack size in fiber is the focus, the propagation of the crack is not considered. Stationary crack can be defined using an enrichment command and assigning crack domain in Abaqus. When the elements are intersected by the defined stationary crack domain, the elastic strength of that element is regarded as zero, which can be regarded as discontinuous.

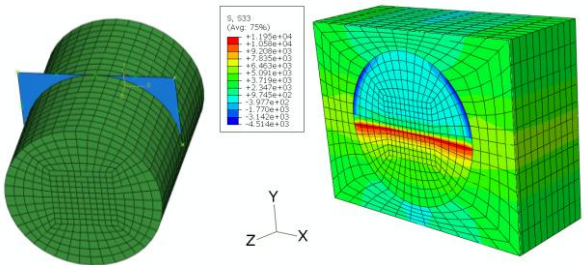

Figure 4-8. Transverse direction crack in fiber.

Figure 4-8 shows the crack in fiber covering the fiber cross section area of 50%. The crack surface has fiber's axial direction and the shape is assumed as half circular. The front of real crack in propagation direction would not have a straight line but it is assumed straight in this research without considering the effect of the crack surface shape for simplicity. The effective stiffness is calculated numerically in the same way as it was calculated for the RVE that does not have crack. Table 4-12 shows how much percentage the stiffness degrades due to the crack when the cracked surface covers 50% of the cross section of the fiber.

Table 4-12. Degradation by transverse direction fiber crack having 50% crack area

+0.56%	-0.27%	-24.52%	0	0	0
-0.22%	+0.54%	-24.80%	0	0	0
-24.17%	-25.75%	-36.58%	0	0	0
0	0	0	+0.77%	-0.11%	0
0	0	0	0	-1.22%	0
-0.01%	-0.01%	-0.49%	0	0	+0.44%

Note that a significant reduction in stiffness is observed in $\bar{E}_{33}$, while $\bar{E}_{11}$ and $\bar{E}_{22}$ are relatively unchanged. The stiffness reduction in Table 4-12 is the case when the crack is appeared periodically, which is not a common expectation of crack in a fiber. Normally, a crack exists only at a specific location, not periodically. Therefore, if the effect of crack is going to be modeled in macro-scale structure, it is necessary to use the reduced stiffness in Table 4-12 only for the location that has a crack. All other locations should use the nominal effective stiffness. In addition, it is important to note that the stiffness reduction in Table 4-12 is proportional to the depth of crack in a fiber.

Homogenization for Inelastic Behavior

When a material shows a nonlinear behavior, its behavior cannot be described using effective stiffness. Instead, a physical model, which comes with model parameters, that describes the behavior of the material is required. Therefore, homogenization of inelastic behavior means to identify the model parameters that make the homogenized material show a similar behavior with the heterogeneous material. In this section, the anisotropic Ramberg-Osgood model is used as a model to describe the inelastic behavior of fiber-matrix composites.

When the fiber is an isotropic elastic material and the matrix is an isotropic hardening elastoplastic material, the fiber reinforced composites behaves like an anisotropic hardening elastoplastic material. Unlike to the elastic behavior, the constitutive relation for elastoplatic material cannot be expressed using one parameter such as stiffness matrix and even becomes more complex when the hardening behavior is anisotropic. Therefore, homogenization is far more complicated than the elastic behavior. As discussed earlier, the UVE, not RVE, is the volume of interest to obtain effective properties for inelastic homogenization. To obtain the properties from UVE, the

appropriate size of the heterogeneous structure should be decided first because the material behavior would be different from the volume element that is placed at the most outer area to the one placed in the middle of the structure.

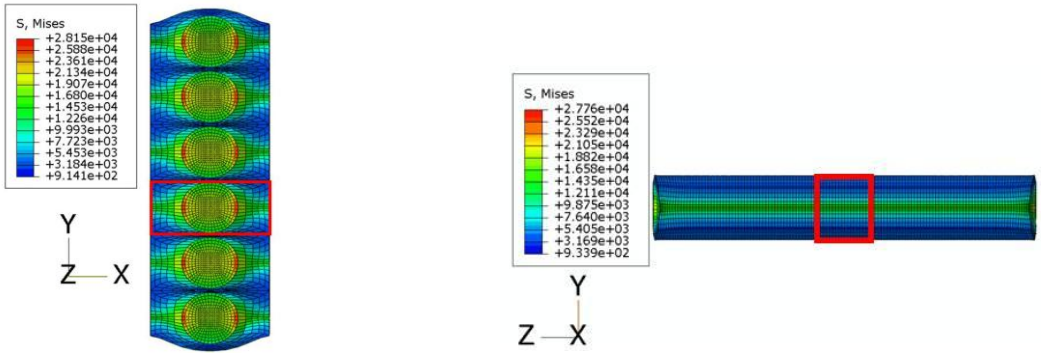

A B

Figure 4-9. Heterogeneous structure composed of UVE piled up. A) Y direction. B) Z direction.

Figure 4-9 shows that the deformed shape of the structures composed of several fibers in y direction and z direction under x direction displacement loading respectively. From Figure 4-9 and Table 4-13, because of symmetry, three of UVEs in y direction pile up seems to be enough for the size of the heterogeneous structure base model and also three of UVEs in z direction would be enough.

Table 4-13. Effective stress in UVE according to their position in each direction

UVE position	Y direction	Z direction
The 3rd UVE (red square)	10.54 MPa	10.32 MPa
The 2nd UVE	10.54 MPa	10.32 MPa
The1st UVE	10.32 MPa	10.21 MPa

The difference in stress values between y direction and z direction come from different geometric constraints. However, the point is three UVE, when symmetry

boundary condition is applied, is enough for the size of the structure. Figure 4-10 shows the heterogeneous structure to be analyzed to obtain effective inelastic properties.

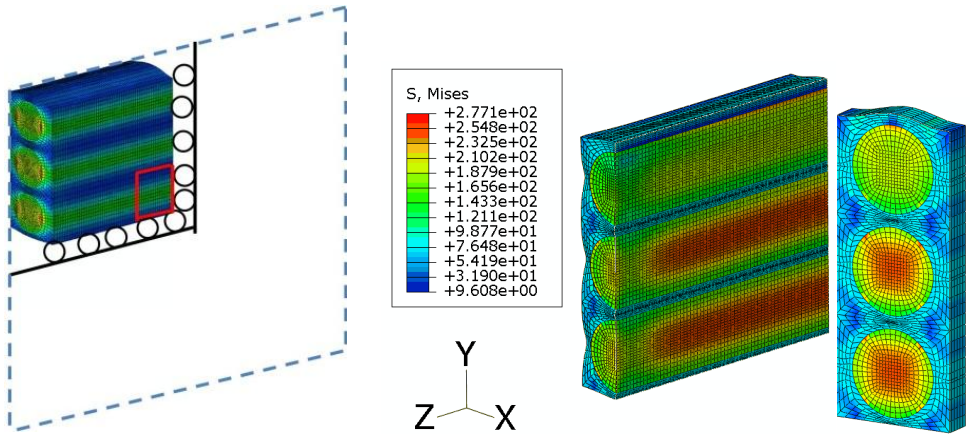

Figure 4-10. Structure to calculate inelastic properties in UVE. A) with a symmetric boundary condition. B) Mises stress distribution in the structure under x direction tension.

As is discussed in Chapter 2, the classical plasticity approach has weakness in terms of the computational cost for homogenization and it is more complicated to model when statistical analysis should be performed. On the contrary, the Ramberg-Osgood model does not require expensive iteration processes to obtain the plastic multiplier which is essential in the classical plasticity model and even the yield surface is not required. In addition, anisotropic hardening application to anisotropic Hill's criteria in the classical plasticity theory is not simple. The Ramberg-Osgood model, which was originally introduced for one dimension nonlinear behavior, has been modified for three dimension applications. But, most of them were for homogeneous material and mostly for the isotropic hardening model. In this research, three-dimensional Ramberg-Osgood model is associated with anisotropic hardening heterogeneous fiber composites so that it can represent the anisotropic behavior of homogenized composite material. The key

to homogenization of multiaxial anisotropic hardening composite material is to obtain Ramberg-Osgood parameters and anisotropy tensor from heterogeneous composite material behavior. Nonlinear least-squares method is used to find optimum values for its parameters so that it has minimum discrepancy with the behavior of heterogeneous material. Anisotropy tensor is originated from the Hill's anisotropy yield criterion. However, the Hills coefficients are found that they are limited in representing anisotropic behavior of RVE, especially when one direction shows strong elastic behavior.

Three-dimension Ramberg-Osgood model

The three-dimensional Ramberg-Osgood model is implemented to Abaqus FE program through the user subroutine coded by FORTRAN. Equation (27) shows the tensor form of anisotropic Ramberg-Osgood model used in this research. The difference from the original Ramberg-Osgood model is that it is written in the tensor form and has an anisotropy tensor, M.

$$\bar{\boldsymbol{\varepsilon}} = \bar{\boldsymbol{H}} : \bar{\boldsymbol{\sigma}} + A\left(\frac{\bar{\sigma}_{eq}}{TY}\right)^{B} \boldsymbol{M} : \bar{\boldsymbol{S}} \tag{27}$$

$\bar{\boldsymbol{\varepsilon}}, \bar{\boldsymbol{\sigma}}$: Effective strain and effective stress

$\bar{\boldsymbol{H}}$: Effective compliance tensor

$\boldsymbol{M}$: Anisotropy tensor to be calculated

$\bar{\boldsymbol{S}}$: Effective deviatoric stress vector

σ_{eq}: Anisotropic equivalent stress

A,TY and B: constants to be calculated

The compliance matrix, $\boldsymbol{S}$, was obtained from the inverse of the effective stiffness matrix obtained from the homogenization procedure for elastic behavior of the RVE.

To calculate equivalent stress which is defined in equation (28), anisotropy tensor should be calculated.

$$\sigma_{eq} = \sqrt{\boldsymbol{S}:\boldsymbol{M}:\boldsymbol{S}} \tag{28}$$

$p = -\frac{1}{3}\boldsymbol{\sigma}:\boldsymbol{I}$ The equivalent hydrostatic stress

$\boldsymbol{S} = \boldsymbol{\sigma} + p\boldsymbol{I}$ The stress deviator

For orthotropic materials, the components of anisotropy tensor, M, can be described by Hill's parameters F, G, H, L, M and N. The Hill's [104] parameters are known as material properties and they are independent on the loading state. The anisotropy tensor in the equation (27) restricted to orthogonal materials but our model has fiber in the center of matrix and the x direction and y direction symmetry made it identical to transversely isotropic materials.

$$[M] = \begin{bmatrix} \mathrm{G}+\mathrm{H} & -\mathrm{H} & -\mathrm{G} & 0 & 0 & 0 \\ -\mathrm{H} & \mathrm{H}+\mathrm{F} & -\mathrm{G} & 0 & 0 & 0 \\ -\mathrm{G} & -\mathrm{G} & \mathrm{F}+\mathrm{G} & 0 & 0 & 0 \\ 0 & 0 & 0 & 2L & 0 & 0 \\ 0 & 0 & 0 & 0 & 2L & 0 \\ 0 & 0 & 0 & 0 & 0 & 2L \end{bmatrix} = \begin{bmatrix} 1 & -1 & 0 & 0 & 0 & 0 \\ -1 & 1 & 0 & 0 & 0 & 0 \\ 0 & 0 & 0 & 0 & 0 & 0 \\ 0 & 0 & 0 & 0.664 & 0 & 0 \\ 0 & 0 & 0 & 0 & 0.664 & 0 \\ 0 & 0 & 0 & 0 & 0 & 0.664 \end{bmatrix} \tag{29}$$

Components in anisotropy tensors can be found from six material tests that are carried out on the heterogeneous UVE FE model. Three uniaxial tensile tests and three uniaxial shear tests in the principal directions are required but symmetry reduced the number of tests. Yield stress ratio R_{ij} is defined by the measured yield stress in particular direction compared to the reference yield stress, σ_0, which is σ_{11} in this research.

$$R_{ij} = \frac{\bar{\sigma}_{ij}}{\sigma_0} = \frac{\bar{\sigma}_{ij}}{\sigma_{11}} \tag{30}$$

From the uniaxial tests, the components are obtained.

$$F = \frac{(\sigma^0)^2}{2}\left(\frac{1}{\bar{\sigma}_{22}^2} + \frac{1}{\bar{\sigma}_{33}^2} - \frac{1}{\bar{\sigma}_{11}^2}\right) = \frac{1}{2}\left(\frac{1}{R_{22}^2} + \frac{1}{R_{33}^2} - \frac{1}{R_{11}^2}\right) = 0 \tag{31}$$

$$G = \frac{(\sigma^0)^2}{2}\left(\frac{1}{\bar{\sigma}_{33}^2} + \frac{1}{\bar{\sigma}_{11}^2} - \frac{1}{\bar{\sigma}_{22}^2}\right) = \frac{1}{2}\left(\frac{1}{R_{33}^2} + \frac{1}{R_{11}^2} - \frac{1}{R_{22}^2}\right) = 0$$

$$H = \frac{(\sigma^0)^2}{2}\left(\frac{1}{\bar{\sigma}_{11}^2} + \frac{1}{\bar{\sigma}_{22}^2} - \frac{1}{\bar{\sigma}_{33}^2}\right) = \frac{1}{2}\left(\frac{1}{R_{11}^2} + \frac{1}{R_{22}^2} - \frac{1}{R_{33}^2}\right) = 1$$

$$L = \frac{3}{2}\left(\frac{\tau^0}{\bar{\sigma}_{23}}\right)^2 = \frac{3}{2R_{23}^2} = 0.332$$

$$M = \frac{3}{2}\left(\frac{\tau^0}{\bar{\sigma}_{13}}\right)^2 = \frac{3}{2R_{13}^2} = 0.332$$

$$N = \frac{3}{2}\left(\frac{\tau^0}{\bar{\sigma}_{12}}\right)^2 = \frac{3}{2R_{12}^2} = 0.332$$

As the reference yield stress is x direction, symmetry in x direction and y direction makes G=0, and the elastic behavior in z direction made F=0. The shear part L, M and N is defined by the relation in Mises criteria, $\tau_0 = \frac{\sigma_0}{\sqrt{3}}$, but this does not apply to the heterogeneous materials behavior. Most of all, Hill's anisotropy parameters are for anisotropic yield point and they do not have any information on anisotropic hardening behavior. Therefore, anisotropic hardening should be included by Ramberg-Osgood parameters and the shearing components in anisotropy tensor can be obtained together when the parameters are calculated through optimization procedure.

Parameters Calculation

First, the heterogeneous composite UVE is modeled using Abaqus, and the stress-strain relation is calculated by gradually increasing strain in each direction. Then, the goal is to find the Ramberg-Osgood model parameters of a homogeneous material that describe a similar behavior with the Abaqus model. The anisotropic multiaxial Ramberg-Osgood model's parameters and anisotropy tensor are obtained using nonlinear least square fit (NLSQ) function in Matlab. The data that Ramberg-Osgood parameters are fitted is obtained from Abaqus FE analysis of UVE in heterogeneous structure in x direction and xy shear direction. The NLSQ finds parameters that minimize the error which is defined as the square sum of the difference between the Abaqus-calculated stress and the stress from the Ramberg-Osgood model at the same strain values (see equation (32)).

$$error = \sqrt{\sum_{1}^{data} \sum_{i=1}^{6} (\sigma_{\mathrm{i}} - \sigma_{\mathrm{ROi}})^2} \tag{32}$$

In addition to the Ramberg Osgood parameters, the anisotropy tensor component, M_{44}, is also calculated from NLSQ instead of using Hill's anisotropy tensor that is calculated at equation (31). All parameters in the model are calculated as optimized values for the Ramberg-Osgood model so that it can represent the behavior of the heterogeneous material model. Table 4-14 shows the optimized Ramberg-Osgood parameters obtained from this procedure for given mechanical property of matrix. SY1 is the first yield point of the matrix material's stress-strain curve and SY2 is the second yield point that matrix material begins perfect plastic deformation.

Table 4-14. Optimized Ramberg Osgood parameters for given matrix materials' properties

#	SY1	SY2	A	TY	B	M44	Error
1	39.75	61.83	7.67E-08	30.06	6.28	3.90	1.85E-01
2		67.40	3.91E-08	27.27	5.95	3.78	1.83E-01
3		70.00	7.48E-08	31.84	5.98	3.81	1.82E-01
4		72.60	7.14E-08	32.29	5.90	3.81	1.81E-01
5		78.17	6.78E-08	32.34	5.55	3.81	1.78E-01
6	43.33	61.83	1.00E-09	20.40	7.50	3.84	1.83E-01
7		67.40	4.16E-08	31.02	6.51	3.82	1.80E-01
8		70.00	7.37E-08	31.85	5.98	3.79	1.78E-01
9		72.60	6.81E-08	32.30	5.90	3.79	1.77E-01
10		78.17	7.76E-08	32.65	5.52	3.74	1.75E-01
11	45.00	1.83	1.00E-09	20.41	7.50	3.83	1.82E-01
12		67.40	1.00E-09	21.00	7.23	3.79	1.79E-01
13		70.00	3.35E-08	31.11	6.49	3.79	1.77E-01
14		72.60	7.03E-08	32.31	5.90	3.79	1.76E-01
15		78.17	7.55E-08	32.65	5.52	3.75	1.74E-01
16	46.67	61.83	1.00E-09	20.88	7.60	3.80	1.82E-01
17		67.40	1.00E-09	21.30	7.29	3.79	1.78E-01
18		70.00	1.00E-09	21.27	7.12	3.76	1.76E-01
19		72.60	7.23E-08	37.55	6.68	3.73	1.75E-01
20		78.17	7.76E-08	32.75	5.53	3.74	1.73E-01
21	50.25	61.83	1.00E-09	22.56	7.98	3.86	1.83E-01
22		67.40	8.02E-08	42.89	8.00	3.77	1.76E-01
23		70.00	8.58E-08	44.42	8.00	3.67	1.75E-01
24		72.60	1.00E-09	22.45	7.19	3.72	1.73E-01
25		78.17	2.76E-08	32.54	6.23	3.73	1.70E-01

To see graphically how close the homogenized model is to the heterogeneous RVE model, the effective stress-strain curves for both cases are compared in Figure 4-11. Each figure has both heterogeneous materials data that is marked by crosses and homogenized Ramberg-Osgood model data marked by circles. Figure 4-11 (a) shows the effective stress in x direction when the x direction displacement is applied to the heterogeneous materials and homogenized materials that has matrix's first yield stress of 39.75MPa (SY1) and (b) of 50.25MPa(SY5) while keeping the second yield stress of 78.17MPa. It corresponds to the comparison between #5 and #25 in Table 4-14.

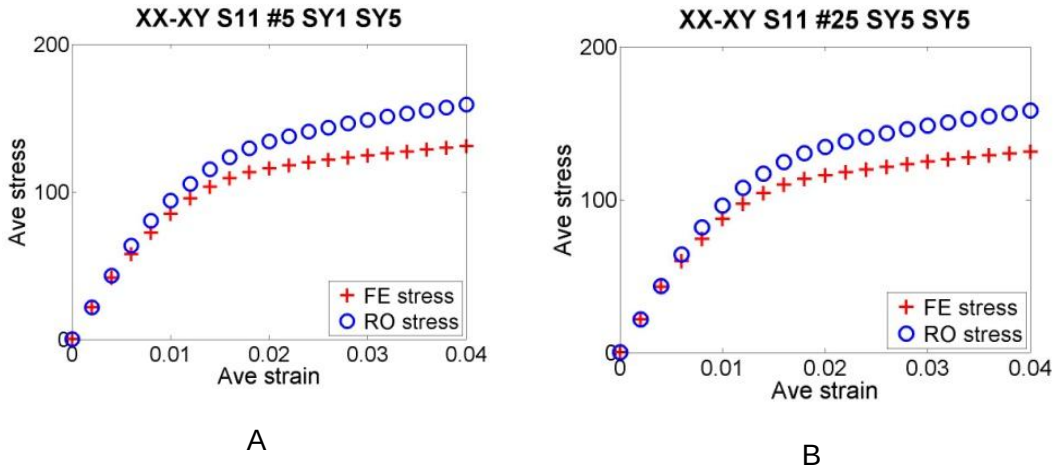

A B

Figure 4-11. X-direction average stress in homogenized material and in heterogeneous material. A) for the first yield stress of 39.75MPa. B) for 50.25MPa.

The elastic region matches well for either case but as the strain increases, the discrepancy also increases. As the Ramberg Osgood parameters are from best curve fit by NLSQ to normal tension data and shear data at the same time, the shear behavior also needs to be verified. Figure 4-12 shows when xy shear displacement is applied for the same model.

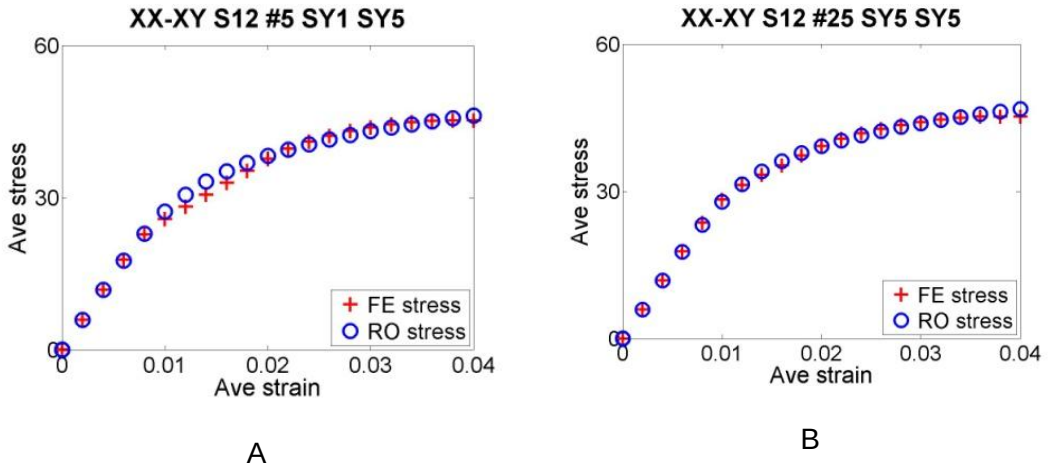

A B

Figure 4-12. XY-shear direction average stress in homogenized material and in heterogeneous material varying the first yield stress.

This shows the optimized Ramberg Osgood model well matches for shear stress-strain relation but a little off in normal loading state. One thing to note is that A) and B) curves are almost identical in both Figure 4-11 and Figure 4-12. It means the variation in the first yield point does not affect the elastoplastic behavior of the composite material.

However, Figure 4-13 shows that the variation of second yield points affects the behavior of materials noticeably.

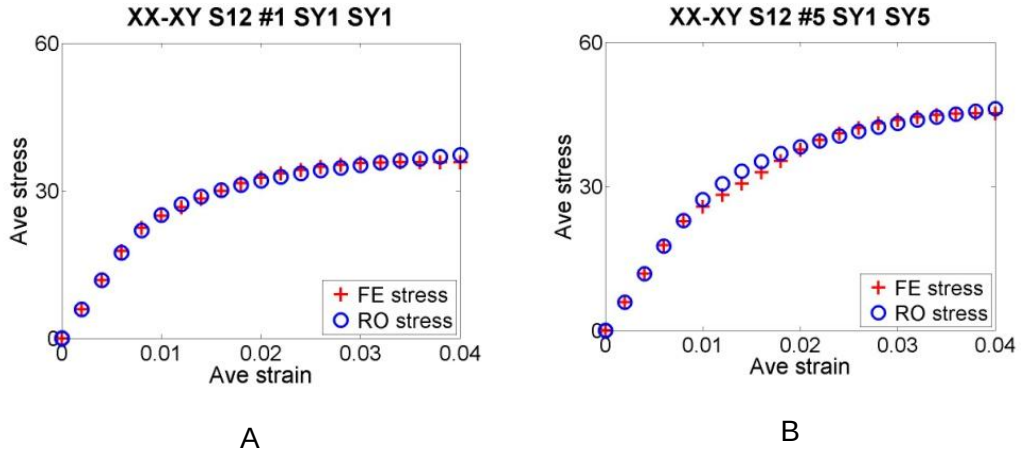

A B

Figure 4-13. XY shear direction average stress in homogenized material and in heterogeneous material varying second yield stress.

As it is proven at this point that the first yield stress of matrix is not critical parameter for macroscopic behavior, it is not considered in uncertainty analysis as an input parameter while the second yield stress is considered.

In contrast to the x and y direction, the composite material behaves almost linear elastic in z direction which is axial direction of fiber. The comparison between heterogeneous materials and homogenized model is shown in Figure 4-14. It shows that the Ramberg-Osgood model can represent linear elastic behavior in z direction accurately and even identical to the composites' behavior.

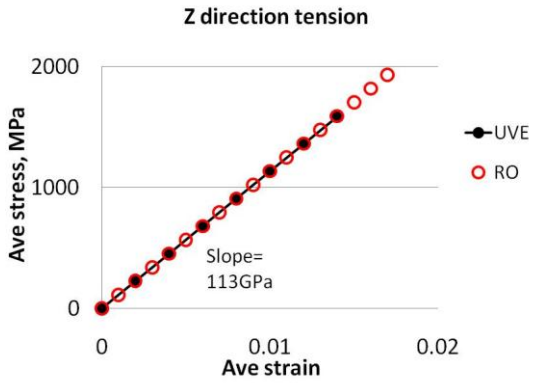

Figure 4-14. Z direction average stress in homogenized material and in heterogeneous material.

Combined Loading Case

The general loading cases in working environment is the combination of the two loading types, normal stress and shear stress. So, the parameters that were obtained under unidirectional tension and unidirectional shear loading should satisfy arbitrary complex loading condition as well when it is homogenized. To verify this, combined loading conditions are applied and compared their behaviors. One is the mixture of shear and tensile displacement loading and the other is biaxial normal loading. For shear and tensile loading mixture, the same amount of displacement is applied to both heterogeneous model that has matrix's first yield stress is 45MPa and second yield stress is 70MPa, and corresponding homogenized model. The shear strain of 0.04 and the tensile strain in x direction of 0.04 are applied at the same time. Figure 4-15 shows the x directions stress contour under the combined loading case compose of shear and tensile loading. The calculation time used for (A) is 12 minutes and for (B) 4 seconds, which is a significant difference considering the size of the analysis.

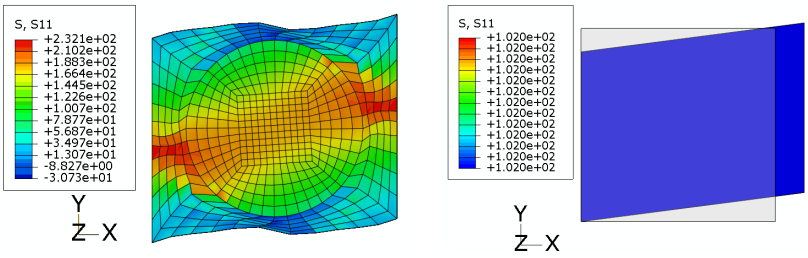

A B

Figure 4-15. Deformed shape and x direction stress under shear and tensile combined loading. A) Heterogeneous materials. B) Homogeneous materials.

However, as the homogenized model has only one element, it cannot make similar deformed shape as heterogeneous materials. However, its effect is important and need to be studied in the future. Figure 4-16 shows that the homogenized model works well in shear and tensile combined loading condition. The elastic behavior of the homogenized material is almost identical to heterogeneous one and the plastic region also shows very similar behavior. The stresses in y direction and z direction are not plotted because they show zero stresses under this loading condition.

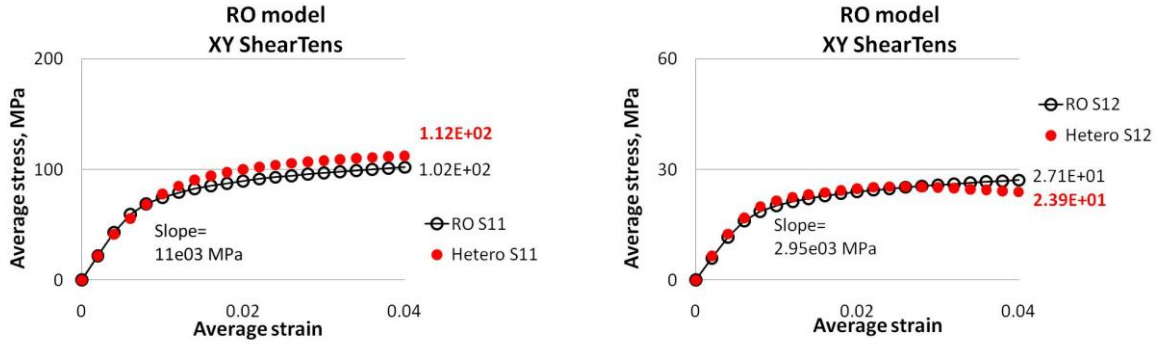

A B

Figure 4-16. Inelastic behavior comparison for heterogeneous and homogenized model. A) X direction average stress under combined load. B) XY shear average stress.

For the verification, another combined loading condition is applied. X direction normal strain of 0.04 and Y direction compressive normal strain are applied to the heterogeneous RVE and homogenized model as well. Figure 4-17 shows the x directions stress contour under biaxial combined loading condition.

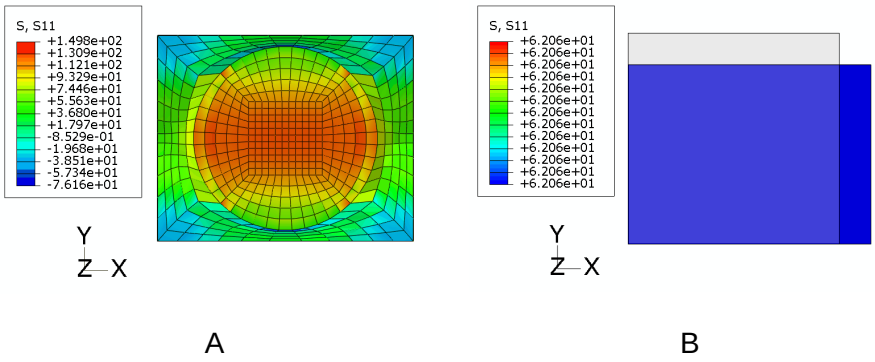

Figure 4-17. Contour of x direction stress under biaxial combined loading. A) Heterogeneous materials. B) Homogeneous materials.

Figure 4-18 shows that the homogenized model works well in biaxial combined loading condition too. From these verifications, it can be said that the homogenized materials using multiaxial anisotropic Ramberg Osgood model behaves very similar to heterogeneous RVE material not only in unidirectional but also in combined loading conditions.

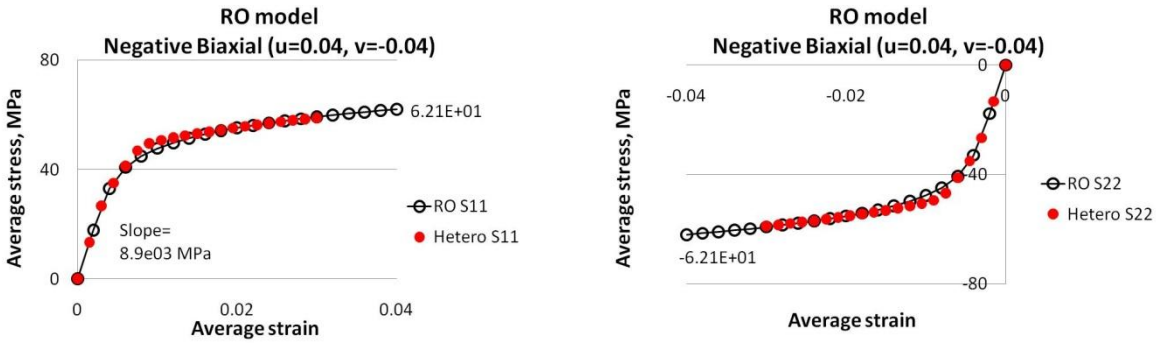

A B

Figure 4-18. Average stress comparison under biaxial loading. A) x direction. B) y direction.

Therefore, the Ramberg-Osgood parameters that are obtained from heterogeneous material data satisfy not only the uniaxial loading but also the elastoplastic stress-strain relation under combined loading states. As we have a homogenized material model, we don't need to run time consuming heterogeneous materials analysis.

CHAPTER 5
UNCERTAINTY ANALYSIS

Introduction

Experimental researches in engineering have shown that model parameters or material properties show a random, or stochastic character no matter what the materials are. Heterogeneous materials such as a composite material have a complex structure and, unfortunately, because of high demand in performance, the micro- or macro-structures become complicated. This causes the uncertainty in parameters relating to the composites to increase. Even in a specific interest of scale, many parameters, such as voids, crack, particles and grain boundaries are involved, but it is not easy to tell how much they are involved in failure or how these parameters may be correlated to one another. The analysis based on exact values that do not take uncertainty into account is called deterministic analysis. On the other hand, the uncertainty analysis considers uncertainty in input parameters and their effects on results. For the uncertainty analysis, material parameters having statistical distribution are used as inputs instead of deterministic values. For uncertainty modeling, the uncertainty in the model inputs should be characterized first. This can be represented by standardized normal random variables (srvs) with zero mean and variance of one.

When other types of random variables are going to be used, a transformation is required. An assumption on the input variables is that they are independent so that each variable can be expressed in terms of srvs through a transformation. When the input variables are ready, uncertainty propagation should be carried out with generated samples of input variables. Monte Carlo Simulation (MCS) is the most common method to generate random samples because of its simplicity in implementing on a computer

program and it does not require specific knowledge of properties. However, it has weakness that it requires large number of samples, on the order of thousands or even millions, to have acceptable precision in the response. This is not appropriate for computationally expensive models because it takes too long to consider all the samples created by MCS especially for FE analysis.

Stochastic Response Surface Method

Response surface method is one of a regression method in statistics. Regression analysis is a statistical method that utilizes the relation between two or more variables in which dependent variables can be estimated by independent variables.

General regression model is shown in equation (1).

$$y = \beta_1 f_1(\mathbf{x}) + \cdots + \beta_p f_p(\mathbf{x}) + \varepsilon \quad (1)$$

As the equation shows, the response is modeled with a combination of functions of variables and error. β_j (i=1,…,p) are the coefficients, $f_j(x)$ (i=1,…p) are the terms or bases and ε is error. The $\mathbf{x}$ indicates a vector of input variables x_1, x_2 and so on. When $f_1(\mathbf{x})$=1 and $f_2(\mathbf{x})$=x, then it is linear (first order) model. When $f_1(\mathbf{x})$=1 and $f_2(\mathbf{x})$=x and $f_p(\mathbf{x}) = x^{p-1}$, then it is a polynomial model.

Both response surface method (RSM) [111] and stochastic response surface method (SRSM) [73] has been used to approximate the output. Stochastic is synonymous with random and often used as counterpart of the word deterministic, and consequently, the SRSM is an extension of RSM that is customized to the random inputs instead of deterministic values.

By transforming all input variables to the standard normal random variables and by using Hermite polynomials, which are orthogonal to the Gaussian distribution, as the

bases functions, the SRSM provides many effective features in identifying probabilistic characteristics of random outputs. It provides robust estimates of the coefficients compared to the one obtained using non-orthogonal polynomials [112] and convergence is optimal for Gaussian processes [113]. The biggest difference of SRSM is the type of input. SRSM uses random variables that have forms of probability density function while RSM uses deterministic values. Through the SRSM, the uncertainty in input parameters propagates to the uncertainty in the response, which is explained in the following step.

The first step for SRSM is to decide which parameters will be input variables and statistically transform them to have standard random variables. As SRSM uses Gaussian distribution, the distribution of the random variable, let say X, can be represented by the transformation [114].

$$X = \mu + \sigma(H_1(\xi)) \tag{2}$$

where μ is the mean of X, σ is the standard deviation of X and $H_1(\xi)$ is the first order orthogonal polynomial of the standard normal distribution ξ, which has a mean of zero and a standard deviation of one. The advantage of this standard normalization is that the same set of orthogonal polynomials can be used for any normal distribution instead of deriving a distribution specific set for each normally distributed parameter.

The second step is to define output approximation. A functional approximation that takes into account all uncertainties in input should be chosen. Polynomial chaos expansion will be used and the collocation point method to select points will be used to obtain the coefficients of the response surface.

The third is to investigate the output of the approximation. As the approximation for the output represented by polynomial expansion is obtained, the statistical

characteristics of the output will be investigated through MCS. The statistical moments, probability density function, and correlation between input and output will be discussed. Since the evaluation of function using SRSM is very inexpensive, millions of samples can be generate to calculate accurate statistical properties of the output.

The SRSM utilizes polynomial chaos expansion to represent the output and the coefficients of the polynomial expansion are calculated using a collocation approach [115]. The procedure is to evaluate the function at several points (and possibly the derivatives of the function) and then fit a polynomial to these known points by minimizing the error between function values and approximations. The coefficients that minimize this error are then found, and the approximation is considered to be a good estimate to the true function [83].

The polynomial expansion in SRSM uses Hermite polynomial bases and provides closed form solution of model output requiring significantly lower number of simulations than MCS. The expression for the 3rd order polynomials in 'n' dimension is shown in equation (3).

$$C^{(3)}(u) = a_0{}^{(3)} + \sum_{i=1}^{n} a_i{}^{(3)} u_i + \sum_{i=1}^{n} a_{ii}{}^{(3)} (u_i^2 - 1) + \sum_{i=1}^{n} a_{iii}{}^{(3)} (u_i^3 - 3u_i) + \sum_{i=1}^{n-1} \sum_{j>1}^{n} a_{ij}^{(3)} u_i u_j + \sum_{i=1}^{n} \sum_{j=1, j\neq i}^{n} a_{ijj}^{(3)} (u_i u_j^2 - u_i) + \sum_{i=1}^{n-2} \sum_{j>i}^{n-1} \sum_{k>j}^{n} a_{ijk}^{(3)} u_i u_j u_k \quad (3)$$

$C^{(3)}(u)$ is the model output, the a_i represent coefficients to be estimated, and 'u' represents standard random variables. The number of unknown coefficients is determined by dimension of the design space 'n' which is the number of random

variables. For 3rd order expansion, the number of unknown can be calculated using equation (4).

$$N^{(3)} = 1 + 3n + \frac{3n(n-1)}{2} + \frac{n(n-1)(n-2)}{6} \quad (4)$$

Although, the procedure using SRSM seems attractive, the challenge is how accurately the polynomial expansion can be established to replace computational model. This includes developing proper method to generate and updating best representative points for surrogate to minimize the error.

Collocation Points

The collocation concept comes from the idea of Gaussian Quadrature in numerical integration [116]. The collocation points are selected based on a modification of the standard orthogonal collocation method. This method is called the orthogonal collocation method [117]. The points are selected so that standard normal random variables, U_i in equation (3) takes the values of either zero or one of the roots of the higher order Hermite polynomial. Those collocations points are in high probability region of the input distribution and it is the feature that makes this kind of effective collocation method cost effective method. The theory behind collocation method is based on the concepts of Gaussian Quadrature. It is a numerical integration technique and uses orthogonal polynomials for the selection of points. Equation (5) is the typical form of integrals in Gaussian Quadrature.

$$\int_F f(x)g(x)dx \quad (5)$$

where g(x) is an orthogonal polynomial and f(x) is a non-negative weighting function defined in the connected space F. Gaussian Quadrature seeks to obtain the best numerical estimate for the integral by choosing x values, evaluating g(x) at the points and computing the integral. The x values are the roots of the orthogonal polynomials. The result of Gaussian Quadrature integration is shown in equation (6).

$$\int_F f(x)g(x)dx \approx \sum_{i=1}^{n} f_i g(x_i) \tag{6}$$

The coefficients depend on the weighing function and g(x) is evaluated at abscissa values that are the roots of the n^{th} orthogonal polynomial calculated with respect to the weighting function f(x). The integral becomes exact when g(x) is a polynomial of degree of 2n-1. It means integral can be estimated using only n samples. Table 5-1shows Hermite Polynomial when the number of unknown value is five and polynomial is 3^{rd} order. The collocation points determine the samples of input variables. Using the selected input variables, which are deterministic values, computational model is used to evaluate the deterministic values of the output. Then, the coefficients of the polynomial expansion can be obtained using the least square method. This is the strength of regression method that presents robust means to estimate coefficients because it uses more points than collocation points. When we have the output represented by a polynomial expansion, not by time consuming computational model, we can use the MCS method using the SRSM to analyze uncertainty propagation. Consequently, we replaced the time consuming computational procedure with polynomial equation to apply MCS that requires huge amount of iterations.

Table 5-1. The third order Hermite polynomial basis for five input variables (P represents the order of polynomial)

Order					
P=0	1				
P=1	u_1	u_2	u_3	u_4	u_5
P=2	u_1^2-1	u_1u_2	u_1u_3	u_1u_4	u_1u_5
	u_2^2-1	u_2u_3	u_2u_4	u_2u_5	
	u_3^2-1	u_3u_4	u_3u_5		
	u_4^2-1	u_4u_5			
P=3	$u_1^3-3u_1$	$u_1^2u_2-u_2$	$u_1^2u_3-u_3$	$u_1^2u_4-u_4$	$u_1^2u_5-u_5$
	$u_1u_2^2-u_1$	$u_1u_2u_3$	$u_1u_2u_4$	$u_1u_2u_5$	
	$u_1u_3^2-u_1$	$u_1u_3u_4$	$u_1u_3u_5$		
	$u_1u_4^2-u_1$	$u_1u_4u_5$			
	$u_1u_5^2-u_1$				
	$u_2^3-3u_2$	$u_2^2u_3-u_3$	$u_2^2u_4-u_4$	$u_2^2u_5-u_5$	
	$u_2u_3^2-u_2$	$u_2u_3u_4$	$u_2u_3u_5$		
	$u_2u_4^2-u_2$	$u_2u_4u_5$			
	$u_2u_5^2-u_2$				
	$u_3^2-3u_3$	$u_3^2u_4-u_4$	$u_3^2u_5-u_5$		
	$u_3u_4^2-u_3$	$u_3u_4u_5$			
	$u_3u_5^2-u_3$				
	$u_4^2-3u_4$	$u_4^2u_5-u_5$			
	$u_4u_5^2-u_4$				
	$u_5^3-3u_4$				

Parametric Design

Parametric model creation of the RVE for the FE analysis is an important technique for uncertainty analysis because building a response surface requires a set of deterministic output data, and it is impractical to make RVEs one by one for every change of variable manually. For example, when the position and size of the fiber in matrix are variables, they can be parameterized in a code that makes a loop to generate several RVE models automatically. The corresponding code in Abaqus is the Python script. A Python script to create RVEs can be written from the scratch but utilizing files

that Abaqus GUI environment generates would save a lot of time for whom the scripts are not familiar. Abaqus GUI by which user makes parts and does analysis clicking menus generate the objective language Python automatically. The files with extension of ‘rec’ and ‘jnl’ are the files written in Python code for temporary and permanently. For example, when elastic modulus of 100GPa and Poisson ratio of 0.3 are given in Abaqus GUI menu, then Abaqus automatically write in a file the following code: mdb.models[‘myModel-1’].materials[‘myMatrl’].Elastic.(table=((100000.0, 0.3),)). Replacing the values to variable and making a loop, each model can be created automatically at every iteration. Figure 5-1 shows examples of RVEs in various geometries of the fibers generated by the parameterized code. The Python code is also used to access and make use of the output data Abaqus calculated during the analysis.

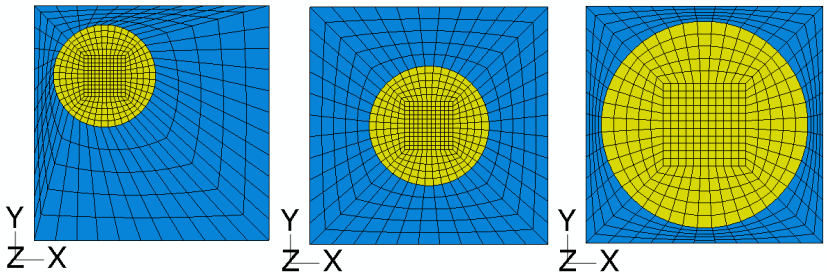

Figure 5-1. Examples of RVE generated by parameterized design.

Uncertainty Propagation in Elastic Behavior

Although there are many parameters in the composite material, three input variables are chosen for calculating the components of the effective stiffness matrix for elastic behavior. First two, Ef and Em, are respectively elastic moduli of fiber and matrix, and Vf is the volume fraction of the fiber. These three variables are the most fundamental ones in the effective properties of composites.

As we have three input variables and applying to 3rd order polynomial, 20 coefficients need to be calculated. The roots of 4th order polynomial, which are $-\sqrt{3+\sqrt{6}}$, $-\sqrt{3-\sqrt{6}}$, $\sqrt{3+\sqrt{6}}$, $\sqrt{3-\sqrt{6}}$ and zero are used as collocation points to fit data to polynomial. This method is called ECM (Efficient Collocation Method) [54].

For collocation points, the three combinations of these roots are used because we need U_1, U_2 and U_3 which represents three random input variables. This result in 5^3(=125) combinations. Generally, more than two times of the unknown parameter is required for the sample number. This means about 40 samples are enough to find 20 unknown coefficients but the number of combination that five collocation points can make is 125. So, we have far more points than we need. Finding efficient way to choose proper 40 points out of 125 could be another study topic but in this research all of 125 points are used to calculate the coefficients using least square fit.

Input Variables for FEM Analysis

In general, the input variables may have different distribution types but for the purpose of SRSM, all input variables are transformed to the standard normal random variables. These input variables are used in SRSM but it should be used in numerical analysis to have physical output values. For the FEM analysis, these input variables should be transformed to have physical meaning, i.e. 100MPa or volume fraction of 0.5. The transformation is performed by a transformation equation that transforms collocation points to the values that has physical meaning.

$$U = f(X) = \frac{X-\mu}{\sigma}, \quad X = U * \sigma + \mu \tag{7}$$

where ‘U’ denotes a standard normal random variable, while ‘X’ the physical input variable. In the above equation, ‘μ’ is the mean and ‘σ’ is the standard deviation of the random variable X. For the following numerical example, the standard deviation of input variable is assumed to be 5% coefficient of variance (COV=σ/μ). The procedure is to find the value of physical variable X for a given collocation point U and statistical parameters μ and σ for the input variable. Then, using the physical variable X, the finite element analysis is performed with the RVE and obtained corresponding data output.

As we input the radius of fiber not the volume fraction of fiber into FEM, we need to find ‘X’ value for the radius to have specific volume fraction. Equation (8) shows the input variables for the radius.

$$R = \sqrt{\frac{1}{\pi}\{U * \sigma_{Vf} + \mu_{Vf}\}} = \sqrt{\frac{1}{\pi}\{U * (COV * \mu_{Vf}) + \mu_{Vf}\}} \quad (8)$$

FE Analysis of the RVE

The stiffness matrix will be calculated putting the deterministic values of the transformed input variables to have physical meaning into the heterogeneous Abaqus RVE model. This was enabled by parameterized design of the RVE. Instead of constructing RVEs for every size of the fiber one by one manually, the radius of the fiber is parameterized so that only changing the value of the radius can construct the corresponding RVE automatically. The mechanical parameter such as fiber’s Young’s modulus and matrix’s Young’s modulus are parameterized too. The geometric parameterization is only possible by the Python code that Abaqus supports.

Table 5-2 shows the input values of parameters that will be put into Abaqus FE analysis to have deterministic output, which is the component of the stiffness matrix. As

each parameter has five values, the combination of all parameters will make total number of 125 FE analysis data. So, each stiffness matrix component has 125 data and it is saved as a vector.

Table 5-2. Input values of parameters for FE anlysis

	#1	#2	#3	#4	#5
Ef	197854.00	215690.00	224000.00	232310.00	250145.00
Em	3091.50	3370.20	3500.00	3629.80	3908.50
Vf	0.44	0.48	0.50	0.52	0.56

Equation (3) can be rephrased to have simpler expression in terms of coefficients and three input variables as

$$\begin{aligned} C= {} & a_0 + a_1(u_1) + a_2(u_2) + a_3(u_3) + a_4(u_1^2 - 1) + a_5(u_1u_2) + a_6(u_1u_3) + a_7(u_2^2 - 1) \\ & + a_8(u_2u_3) + a_9(u_3^2 - 1) + a_{10}(u_1^3 - 3u_1) + a_{11}(u_1^2u_2 - u_2) + a_{12}(u_1^2u_3 - u_3) \\ & + a_{13}(u_1u_2^2 - u_1) + a_{14}(u_1u_2u_3) + a_{15}(u_1u_3^2 - u_1) + a_{16}(u_2^3 - 3u_2) \\ & + a_{17}(u_2^2u_3 - u_3) + a_{18}(u_2u_3^2 - u_2) + a_{19}(u_3^3 - 3u_3) \end{aligned} \quad (9)$$

As we have {c} obtained from FE analysis and input variables $\{U_i\}$ in equation (9), we can calculate its coefficients by matrix algebra and we can have stiffness matrix components expressed in form of polynomial expansion. As long as we have this polynomial expansion for stiffness matrix components, Monte Carlo Simulation can be applied to the expansion for the statistical investigation for the propagation of uncertainty. Table 5-3 shows the twenty coefficients for six stiffness components calculated by least square fit method.

Table 5-3. Coefficients of polynomial expansion for stiffness matrix components

Bases	C11	C12	C13	C33	C44	C55
1	13.517	4.116	4.500	115.615	2.833	3.901
u_1	0.030	0.004	0.008	5.581	0.003	0.008
u_2	0.646	0.202	0.217	0.200	0.139	0.187
u_3	0.943	0.076	0.200	5.565	0.149	0.275
u_1^2	-0.001	0	0	0	0	0
$u_1 u_2$	0.003	0	0.001	0	0	0.001
$u_1 u_3$	0.006	0	0.001	0.280	0	0.001
u_2^2 -1	-0.001	0	0	0	0	0
$u_2 u_3$	0.042	0.004	0.009	-0.001	0.007	0.013
u_3^2 -1	0.060	0	0.012	0.004	0.009	0.017
$\mathrm{u}_1^3 - 3u_1$	0	0	0	0	0	0
$u_1^2 u_2 - u_2$	0	0	0	0	0	0
$u_1^2 u_3 - u_3$	0	0	0	0	0	0
$u_1 u_2^2 - u_1$	0	0	0	0	0	0
$u_1 u_2 u_3$	0.001	0	0	0	0	0
$u_1 u_3^2 - u_1$	0.001	0	0	0	0	0
$\mathrm{u}_2^3 - 3u_2$	0	0	0	0	0	0
$u_2^2 u_3 - u_3$	0	0	0	0	0	0
$u_2 u_3^2 - u_2$	0.002	0	0	0	0	0.001
$\mathrm{u}_3^3 - 3u_3$	0.004	0	0.001	0.002	0.001	0.001

Monte Carlo Simulation

To see the propagation of uncertainty, 50,000 samples from the normally distributed random variables are generated in Matlab and used to calculate the output of stiffness matrix component values from polynomial. Then, using 50,000 values of calculated components, the mean and COV of the output are calculated. Table 5-4 shows the comparison between input COV and output COV. The COV of input variables (Ef, Em and Vf) was equally 0.05, which means the degree of dispersion of those three input variables were same. But, the output shows the degree of dispersion is different.

The stiffness matrix component C33 shows the least variation while C11 and C55 show the most variation, which means uncertainty in input variables propagated most.

Table 5-4. Output statistics of polynomial expansion

Method	Statistics	C11	C12	C13	C33	C44	C55
SRSM	Input COV			0.05			
MCS (Ef, Em, Vf)	Output COV	0.09	0.05	0.07	0.04	0.07	0.09

Thus, we can pay more attention on the C55 direction shearing stiffness when we design uniaxial fiber composites considering modulus of constituents and volume fraction of fiber. Figure 5-2 is the histogram stiffness matrix components and shows how each component is distributed in range.

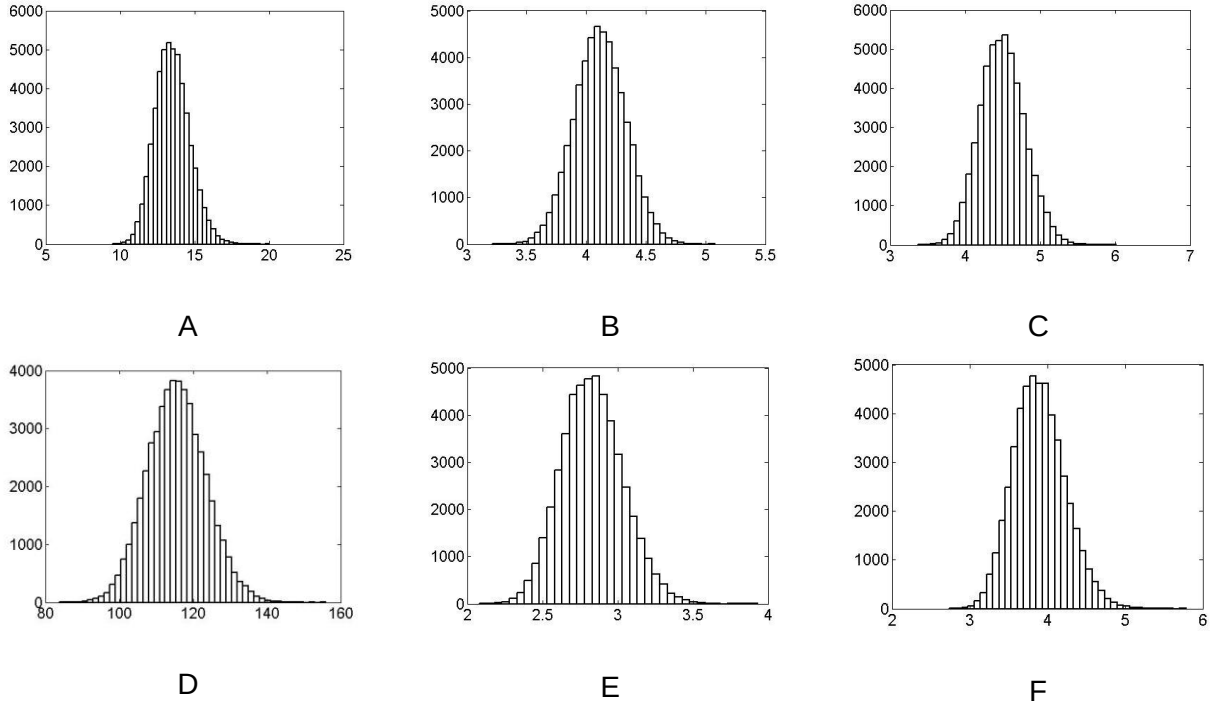

Figure 5-2. Histogram of stiffness matrix component. A) C11. B)C12. C)C13. D)C33. E)C44. F)C55.

Although some COV values are increased from 5% to 9%, the uncertainty in the micro-scale does not amplified much in the macro-scale response. This can be understood if the scaling-up process is considered as an integration process and the

fluctuation in the local material properties are averaged out after integration. Thus, the COV of the macro-scale properties remains in the same level with the micro-scale properties. However, this is only true when both materials are linear elastic.

Uncertainty Propagation in Inelastic Behavior

For elastic behavior of the heterogeneous RVE, it was described by an effective stiffness matrix and each component was expanded into polynomial expression for statistical investigation. However, the elastoplastic behavior of the heterogeneous RVE which is modeled using multiaxial anisotropic Ramberg-Osgood model, has four parameters, which were A, TY, B and M_{44}. These parameters are dependent each other that they could not be described as one values such as an effective stiffness matrix component in elastic condition. For this reason, each parameter cannot be expanded into polynomial expansion independently. Therefore, instead of analysis on the Ramberg-Osgood parameters, the strain energy stored in loading direction is considered in uncertainty analysis.

Input Variables for FEM Analysis

The same input variables as the previous elastic analysis are considered first. The Young's modulus of fiber, the Young's modulus of matrix and the volume fraction of the fiber are verified first. As it has same number of input variables and degree of polynomial, same collocations points are transformed to physical values and put into the Abaqus heterogeneous RVE model. Before calculating deterministic values of strain deformation energy, the elastoplastic behaviors of the heterogeneous RVE were investigated. Figure 5-3 shows that how the heterogeneous RVE behaves in inelastic region when the Young's modulus of fiber, the Young's modulus of matrix and volume fraction change. First, the only difference between A) with C) is the Young's modulus of

fiber, but two curves are identical. The RVE in A) and D) have different Young's modulus of matrix and the curves are not significantly different. This means the uncertainty in Young's modulus of fiber and matrix in this range will not propagate much into the uncertainty of deformation energy. On the contrary, it clearly shows that the volume fraction of fiber makes change in the macro scale response. Figure 5-4 shows the Young's modulus of fiber affects the behavior of the heterogeneous RVE in z direction, which shows a similar trend with Figure 5-3.

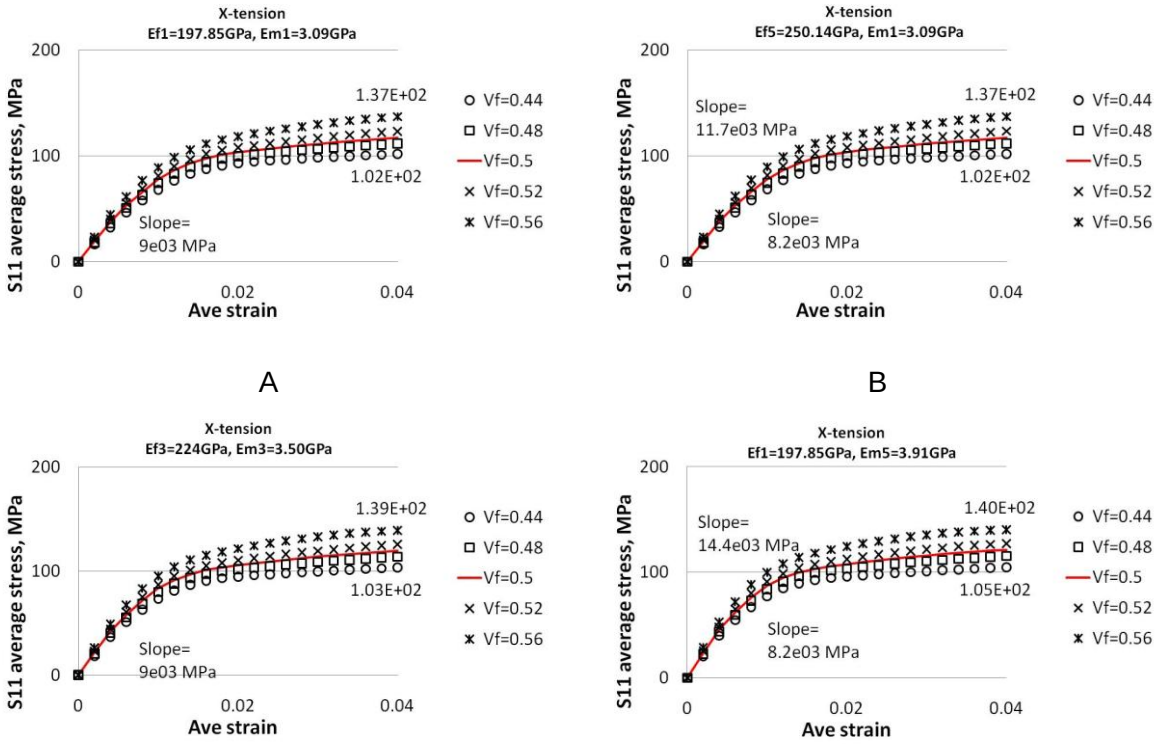

Figure 5-3. Elastoplastic behavior of heterogeneous material according to Young's modulus of fiber and matrix and volume fraction of fiber. A) Ef1=197.85GPa, Em1=3.09GPa. B) Ef5= 250.14GPa, Em1=3.09GPa. C) Ef3=224.00GPa, Em1=3.50GPa. D) Ef1=197.85GPa, Em5=3.91GPa.

Therefore, it is concluded that Young's moduli would not affect much on the inelastic behavior of homogenized material, whereas the volume fraction shows the largest contribution to the output variation.

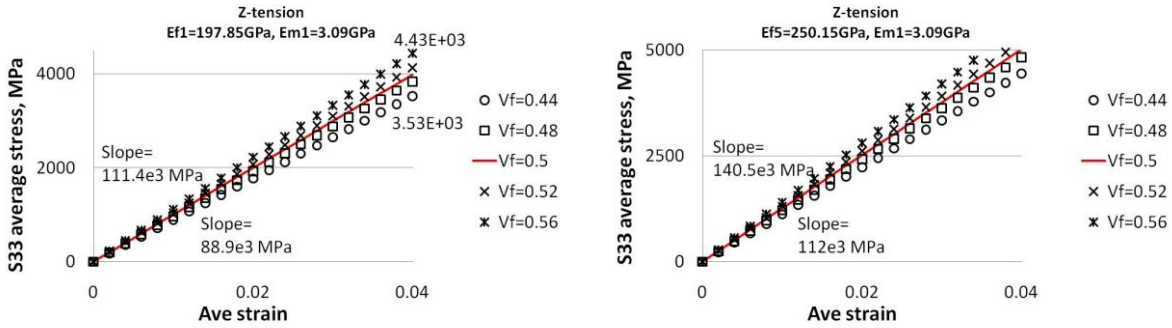

A B

Figure 5-4. Z direction behavior of heterogeneous RVE. A) Ef1=197.85GPa, Em1=3.09GPa. B) Ef5= 250.15GPa, Em1=3.09GPa.

Thus, two input variables are chosen for uncertainty analysis in elastoplastic behavior: fiber volume fraction, Vf, and second yield point of the matrix, SY2.

First, for the volume fraction, the collocation points are transformed to physical values using the transformation equation used before and then so does the second yield point of the matrix. Table 5-5 shows the physical input variables that will be put into Abaqus heterogeneous RVE model.

Table 5-5. Input values of parameters for elastoplastic behavior

	#1	#2	#3	#4	#5
Vf	0.44	0.48	0.5	0.52	0.56
SY2	61.83	67.40	70.0	72.60	78.17

FE analysis of the RVE in Elastoplastic Behavior

X-direction strain energy under x-tension displacement loading (3rd order polynomial with two variables) can be expanded into polynomial as

$$Exx = a_1 + a_2U_1 + a_3U_2 + a_4(U_1^2 - 1) + a_5(U_1 * U_2) + a_6(U_2^2 - 1) +$$

$$a_7(U_1^3 - 3 * U_1) + a_8(U_1^2 * U_2 - U_2) + a_9(U_1 * U_2^2 - U_1) + a_{10}(U_2^3 - 3 * U_2) \quad (10)$$

We have 25 points of design of experiment for 10 unknown coefficients of polynomial. The least square method is used to calculate coefficients.

In a similar way, three kinds of loading conditions are applied, which are x direction tension displacement, xy-shear displacement and xy shear-tension combined displacement condition. The x direction strain energy is calculated for x direction loading and xy shear direction strain energy is calculated for xy shear loading and so on.

When the coefficients are obtained, MCS is performed to estimate the distribution of the output response which is the strain energy in each direction.

Using deterministic data from Abaqus FE analysis, the coefficients polynomial response surface for each loading conditions are calculated and shown in Table 5-6.

Table 5-6. The coefficients of polynomial expansion for strain energy in x direction

	a_0	a_1	a_2	a_3	a_4	a_5	a_6	a_7	a_8	a_9
X tension	3.707	0.131	0.222	-0.002	0.007	0.013	0	0	0.001	-0.001
XY shear	1.243	0.039	0.021	-0.001	0.002	0	0	0	0	0
Combined (tension, shear)	3.506	0.127	0.214	-0.002	0.007	0.014	0	0	0	0
	0.858	0.038	-0.001	0	0.002	-0.001	-0.001	0	0	0

Monte Carlo Simulation

To investigate the propagation of uncertainty, 50,000 samples from the normally distributed random variables are generated in Matlab and used to calculate the output of strain energy in each direction.

Table 5-7. The propagation of the uncertainty for elastoplastic behavior

	Input COV (Vf, SY2)	Output COV (Energy)
X tension	0.05	0.07
XY shear	0.05	0.04
Combined (tension, shear)	0.05	0.07 (x normal direction) 0.04 (xy shear direction)

Table 5-7 and Figure 5-5 shows that the uncertainty in volume fraction and second yield point of the matrix propagated increasing the x direction strain energy but not significantly. It seems the uncertainty in volume fraction and the second yield point propagates to the strain energy without being changed.

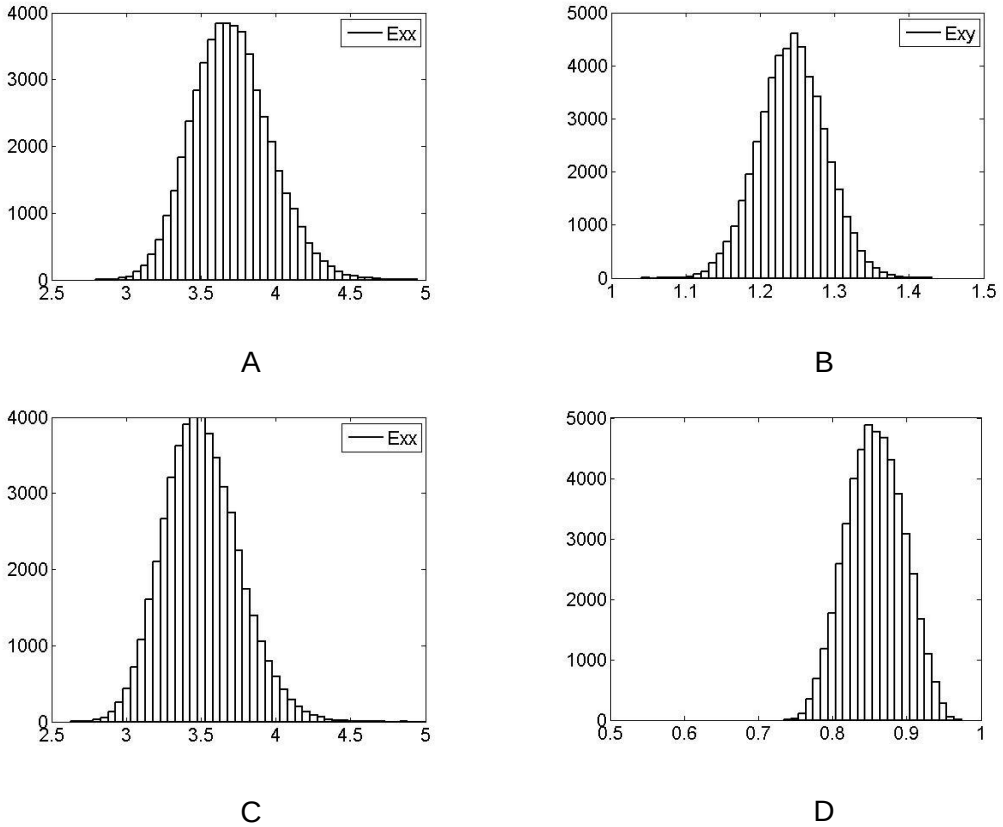

Figure 5-5. Histogram of strain energy for each loading condition in elastoplastic behavior. A) x direction under x tension. B) xy shear direction under xy shear load. C) x direction under combined load. D) xy direction under combined load.

CHAPTER 6
SUMMARY AND CONCLUSIONS

A homogenization method is proposed to reduce the computation cost for fiber reinforced composite material simulation. Not only for elastic behavior but also elastoplastic behavior was homogenized so that both have same average stress-strain constitutive relations. The elastic behavior of the fiber reinforced composites was homogenized through the RVE concept and the effective elastic mechanical properties were obtained by numerical approach using the user subroutine in Abaqus FE program. The application of RVE concept and homogenization in this research has significant meaning in that it significantly reduces computational time, especially for elastoplastic behavior analysis. The Ramberg-Osgood model parameters are successfully calculated from heterogeneous material's FE data using least square fit to find optimal values. The successful implementation of the multi axial anisotropic hardening Ramberg Osgood model into Abaqus FE program made it possible the fast and effective homogenization for inelastic behavior. Through numerical examples, it is shown that the proposed model works well with combined loading conditions not to mention simple uniaxial tension and shear loadings. However, there was a little discrepancy in normal direction behavior while shear behavior matched identical to heterogeneous materials. It seems some coupling between normal and shear direction occurs for combined loading for heterogeneous.

However, it is shown that the boundary condition is important in RVE analysis for periodic heterogeneous materials. The results shows strong dependency on the boundary condition and it needs to be studied more in further researches. In this research, UVE model is used instead of RVE with periodic boundary condition. It could

be said that the boundary condition must be studied deeply when the research is on multi scale analysis.

As the homogenized model in this research is simple compared to complexity of real composite materials, it is possible that important factors and properties can be blurred and buried under homogenization. Although it is true, consideration of applying homogenization should not be disregarded because full scale analysis is still impractical and design and manufacturing requires computational tools. More than that, it is shown that it is practical and worth to studied more.

For uncertainty analysis, Young's modulus of fiber and matrix, volume fraction of fiber, and yield points of matrix were investigated to see how much of the uncertainty in them will propagate to macro behavior of homogenized composites. For elastic behavior, the uncertainty in those parameters propagated to the axial direction stiffness increasing the uncertainty while it did not in other directions. For elastoplastic behavior, among the input variables that considered in this research, the first yield point of matrix part and Young's modulus of both fiber and matrix did not give much effect on the strain energy variation during inelastic deformation. But the uncertainty in volume fraction and second yield point of matrix part propagated to the uncertainty in strain energy when it is under normal direction tension loading. Although the amplification of the uncertainty to macro behavior was not significant, it was enough to make it possible to distinguish which parameters give more effect on the behavior of the material in specific condition.

The homogenization which is oriented to a specific purpose can save computational cost or time significantly and enables bigger scale analysis. Along with homogenization, the uncertainty analysis can reduce the time spent on trial-and-error

and the time spent on finding which parameter should have more attention in design or manufacturing process.

If experimental data was obtainable for this research, it would provide better information. Although the experiment data is essential, it is worth to note that the detail investigation for micro scale using SEM or TEM in experiments only reveals the response, not providing much about mechanism. This means it is possible to choose wrong parameters or miss critical parameters when micromechanics are applied. When more reliable and accurate uncertainty analysis is possible, it could present more accurate information than the one based on experimental data or experiences of individual engineers.

APPENDIX
PYTHON CODE FOR PARAMETRIC ANALYSIS

```
#
# To run the Python when you start Abaqus/CAE
#      type the following command in command line in Abaqus/CAE
#      >>abaqus cae script=***.py
# or to run a script file from the Abaqus command line interface
#      >>execfile('***.py')
# ==========================================
# Parametric study WITH periodic displacement BC (using *equation)
# ==========================================
from part import *
from material import *
from section import *
from assembly import *
from step import *
from interaction import *
from load import *
from mesh import *
from job import *
from sketch import *
from visualization import *
from connectorBehavior import *
from math import *
from Numeric import *
# ****************************************************
# Define mechanical properties and variables
# ****************************************************
fYoung=[179200, 224000, 268800]
nuf=0.3
mYoung=[2800, 3500, 4200]
num=0.26
# Width of RVE
w=1.0
# Fiber center(cx,cy)
cxr=[0.0, 0.02, 0.05]
cyr=[0.0, 0.02, 0.05]
#Volume fraction(=Vf/V, V=1 and Vf=4*pi*R^2*1)
Vfr=[0.4,0.5,0.6]
# Cosine 45 (radian)
```

```
c45=cos(45*pi/180)
# ----------------------------------------------------------------------------
# Define a function to create Uniaxial Fiber Reinforced Composites
def createPartRVE(myModel, Em, Ef, Vf):
# ----------------------------------------------------------------------------
# Define a function to apply the constant in Periodic Displacement Boundary Conditions
def CEqApply(flname, direction, dof):
# ----------------------------------------------------------------------------
# Define a function to apply the Periodic Displacement Boundary Conditions
def CEq(flname, direction):
# ----------------------------------------------------------------------------
#def ends
# ******************************************************
#                       Analysis loop
# ******************************************************
volume=0
iter=1
iter1=1
iter2=1
iter3=1
for Em in mYoung:
        for Ef in fYoung:
                for Vf in Vfr:
                        for cx in cxr:
                                for cy in cyr:
                                    ...
                                    ...
                                    # ----------------------------------------------------------------------------
                                    #                       calcualte average stress
                                    # ----------------------------------------------------------------------------
                                        def aveS(Nframe, filename, stepname):
                                        ...
                                        ...
                                        iter=iter+1
                                        #end of cy loop
                                # end of cx loop
                                # no iteration for cx and cy
                        #end of Vf for loop
                        iter1=iter1+1
                #end of  Ef for loop
```

```
                iter2=iter2+1
            #end of Em for Loop
            iter3=iter3+1
del mdb.models['Model-1']
```

LIST OF REFERENCES

[1] S.T. Peters, Handbook of composites, second edition, Chapman & Hall, New York, 1998.

[2] S.T. Peters, Handbook of composites, Process research, Chapman & Hall, second ed.,1998.

[3] B. Ravi Deo, Strarnes H. James, Jr., Holzwarth C. Richard, Low-cost composite materials and structures for aircraft applications, RTO Applied Vehicle Technology Panel (AVT) Specialists' Meeting, Norway, 7-11 May, 2001.

[4] H. Wittich, K. Friedrich, Interlaminar fracture energy of laminates made of thermoplastic impregnated fiber bundles, Journal of Thermoplastic Composite Materials 1 (1988) 221-231.

[5] Harris E. Charles, Starnes H. James, An assessment of the state-of-the-art in the design and manufacturing of large composite structures for aerospace vehicles, NASA/TM-2001-210844 (2001) 20.

[6] G. D. Wyss, K. H. Jorgensen, A user's guide to LHS: Sandia's latin hypercube sampling software, Sandia National Laboratories, Albuquerque, New Mexico, 1998.

[7] H. Berger, U. Gabbert, H. Koppe, R. Rodrguez-Ramos, J. Bravo-Castillero, R. Guinovart-Diaz, J.A. Otero, G.A. Maugin, Finite element and asymptotic homogenization methods applied to smart composite materials, Computational Mechanics 33 (2003) 61-67.

[8] Jorg Hohe, Wilfried Becker, Effective stress strain relations for two dimensional cellular sandwich cores: Homogenizations, material models and properties, Appl. Mech. Rev. 55 (2002) 61-87.

[9] J.D. Eshelby, The determination of the field of an ellipsoidal inclusion and related problems, Proc. R. Soc. Lond. A 241 (1957) 376-396.

[10] Z. Hashin, The elastic moduli of heterogeneous materials, J. Appl. Mech. 29 (1962) 143-150.

[11] T. Mori, K. Tanaka, Average stress in the matrix and average elastic energy of materials with misfitting inclusions, Acta Metall. 21 (1973) 571-574.

[12] W. Voigt, On the relation between the elasticity constants of isotropic bodies, Ann. Phys. Chem. 274 (1889) 573–587.

[13] A. Reuss, Determination of the yield point of Polycrystals based on the yield condition of single crystals, Z. Angew. Math. Mech. 9 (1929) 49–58.

[14] R. Hill, A self-consistent mechanics of composite materials, J. Mech. Phys. Solids 13 (1965) 357-372.

[15] R. M. Christensen, K.H. Lo, Solution for effective shear properties in three phase sphere and cylinder models, J. Mech. Phys. Solids 27 (1979) 315-330.

[16] R. Hill, The elastic behaviour of a crystalline aggregate, Proc. R. Soc. London, Ser. A 65 (1952) 349–354.

[17] A. Benssousan, J.L. Lions, G. Papanicoulau, Asymptotic analysis for periodic structures, North-Holland, 1978.

[18] Sanchez-Palencia, Non-homogeneous media and vibration theory, Lecture notes in physics127, Springer-Verlag, Berlin, 1980.

[19] J. M. Guedes, N. Kikuchi, Preprocessing and post processing for materials based on the homogenization method with adaptive finite element methods, Computer Methods in Applied Mechanics and Engineering 83 (1990) 143-198.

[20] K. Terada, N. Kikuchi, Nonlinear homogenization method for practical applications, Computational Methods in Micromechanics, ASME, New York, AMD-212/MD-62 (1995) 1-16.

[21] J. Fish, K. Shek, M. Pandheeradi, M.S. Shephard, Computational plasticity for composite structures based on mathematical homogenization: Theory and practice, Comp. Meth. Appl. Mech.Engng. 148 (1997) 53-73.

[22] J. Fish and K. L. Shek, Finite deformation plasticity of composite structures: Computational models and adaptive strategies, Comp. Meth. Appl. Mech. Engng. 172 (1999) 145-174.

[23] J. Fish, Q.Yu, Multiscale damage modeling for composite materials: Theory and computational framework, International Journal for Numerical Methods in Engineering 52(1-2) (2001) 161-192.

[24] Terada, K., Kikuchi, N., A class of general algorithms for multi-scale analysis of heterogeneous media, Comput. Methods Appl. Mech. Eng. 190 (2001) 5427-5464.

[25] K. Matsui, K. Terada, K. Yuge, Two-scale finite element analysis of heterogeneous solids with periodic microstructures, Computers and Structures 82 (2004) 593-606.

[26] R.J.M. Smit, W.A.M. Brekelmans, H.E.H. Meijer, Prediction of the mechanical behavior of nonlinear heterogeneous systems by multilevel finite element modeling, Comput. Methods Appl. Mech. Eng. 155 (1998) 181-192.

[27] C. Miehe, A. Koch, Computational micro-to-macro transition of discretized microstructures undergoing small strain, Arch. Appl. Mech. 72 (2002) 300-317.

[28] V. Kouznetsova, W.A. Brekelmans, F.P.T. Baaijens, , An approach to micro-macro modeling of heterogeneous materials, Comput. Mech. 27 (2001) 37-48.

[29] F. Feyel, J.L. Chaboche, FE2 multiscale approach for modeling the elasto-viscoplastic behavior of long fiber sic/ti composite materials, Comput. Methods Appl. Mech. Eng. 183 (2000) 309-330.

[30] S. Ghosh, K. Lee, S. Moorthy, Multiple scale analysis of heterogeneous elastic structures using homogenization theory and Voronoi cell finite element method, Int. J. Solids Struct. 32 (1995) 27-62.

[31] S. Ghosh, K. Lee, S. Moorthy, Two scale analysis of heterogeneous elasticplastic materials with asymptotic homogenization and Voronoi cell finite element model. Comput. Methods Appl. Mech. Engrg. 132 (1996) 63-116.

[32] J.C. Michel, H. Moulinec, P. Suquet, Effective properties of composite materials with periodic microstructure: a computational approach, Comput. Methods Appl. Mech. Eng. 172 (1999) 109-143.

[33] M.G.D. Geers, V. Kouznetsova, W.A.M. Brekelmans, Gradient-enhanced computational homogenization for the micro-macro scale transition, J. Phys. IV 11 (2001) 145-152.

[34] C. McVeigh, F. Vernerey, W. K. Liu, L. C. Brinson, Multiresolution analysis for material design, Comput. Methods Appl. Mech. Engrg. 195 (2006) 5053–5076.

[35] Derek Hulk, T.W, Clyne, An Introduction to composite materials, Cambridge University Press. 1996.

[36] P. Sharma, S. Ganti, Size-dependent Eshelby's tensor for embedded nano-inclusions incorporating surface/interface energies, Journal of Applied Mechanics 71(5) (2004) 663–671.

[37] S.Li, R.A. Sauer, G. Wang, A circular inclusions in a finite domain I. The Dirichlet-Eshelby problem. Acta Mech. 179 (2005) 67-90.

[38] R. Hill, Elastic properties of reinforced solids: Some theoretical principles, J. Mech. Phys. Solids 2 (1963) 357-372.

[39] A. A. Gusev, Representative volume element size for elastic composites: A numerical study, Mech. Phys. Solids 45 (1997) 1449-1459.

[40] S. Hazanov, M. Amieur, On overall properties for elastic heterogeneous bodies smaller than the representative volume, Int. J. Engnr Sci. 33(9) (1995) 1289-1301.

[41] B.R. Kima, H.K. Lee, An RVE-based micromechanical analysis of fiber-reinforced composites considering fiber size dependency, Composite Structures 90 (4) (2009) 418-427.

[42] M.W. Hyer, A.M. Waas, Micromechanics of linear elastic continuous fiber composites, Reference Works, Comprehensive Composite Materials, Elsevier, 2000.

[43] Z. Hashin, BW. Rosen, The elastic moduli of fibre-reinforced materials, ASME, Journal of Applied Mechanics 31 (1964) 223-232.

[44] G. Caligiana, F. Cesari, I materiali compositi, Pitagora Editrice, Bologna, 2002.

[45] S. Li, On the unit cell for micromechanical analysis of fibre-reinforced composites, Proceedings Royal Society London, A 455 (1999) 815-38.

[46] D.F. Adams, D.A. Crane, Finite element micromechanical analysis of a unidirectional composite including longitudinal shear loading, Computers and Structures 18 (1984) 1153-65.

[47] D.F. Adams, D.R. Doner, Longitudinal shear loading of a unidirectional composite, Journal of Composite Materials 1 (1967) 4-17.

[48] D.S. Li, M.R. Wisnom, Finite element micromechanical modeling of unidirectional fibre reinforced metal-matrix composites, Compos Sci. Technol. 51 (1994) 545-63.

[49] M.R. Nedele, M.R. Wisnom, Finite element micromechanical modeling of a unidirectional, composite subject to axial shear loading, Composites 25 (1994) 263-272.

[50] S. Li, General unit cell for micromechanical analyses of unidirectional composites, Composites Part-A 32 (2000) 815-816.

[51] Marek Jerzy Pindera, Jacob Aboudi, Steven M. Arnold, Limitations of the uncoupled, RVE-based micromechanical approach in the analysis of functionally graded composites, Mechanics of Materials 20 (1995) 77-94.

[52] R. Hill, Elastic properties of reinforced solids: Some theoretical principles, J. Mech. Phys. Solids 11 (1963) 357-372.

[53] Satish Bapananalli, Ba Nghiep Nguyen, Prediction of elastic properties for curved fiber polymer composites, Polymer Composites (2008) 544-550.

[54] Zihui Xia, Yunfa Zhang, Fernand Elly, A unified periodical boundary conditions for representative volume elements of composites and applications, International Journal of Solids and Structures 40 (2003) 1907–1921.

[55] G. Mathan, N. Siva Prasad, Evaluation of effective material properties of spiral wound gasket through homogenization, International Journal of Pressure Vessels and Piping 87 (2010) 704-713.

[56] Yi Pan, Lucian Iorga, Assimina A. Pelegri, Analysis of 3D random chopped fiber reinforced composites using FEM and random sequential adsorption, Computational Materials Science 43 (2008) 450–461.

[57] Anthony Drago, Marek-Jerzy Pindera, Micro-macro mechanical analysis of heterogeneous materials: Macroscopically homogeneous vs periodic microstructures, Composites Science and Technology 67 (2007) 1243–1263.

[58] L. Capolungo, C. Jochum, Homogenization method for strength and inelastic behavior of nanocrystalline materials, International Journal of Plasticity 21 (2005) 67–82.

[59] P. Luciano Moreira, Gerard Ferron, Finite element implementation of an orthotropic plasticity model for sheet metal forming simulations, Latin American Journal of Solids and Structures 4 (2007) 149-176.

[60] G. Mathan, N. Siva Prasad, Evaluation of effective material properties of spiral wound gasket through homogenization, International Journal of Pressure Vessels and Piping 87 (2010) 704-713.

[61] Brett A. Bednarcyk, Marek Jerzy Pindera, Inelastic response of a woven carbon/copper composite-PartII: Micromechanics model, Journal of composite materials 34 (2000) 299-331.

[62] Zhenyu Xue, Ashkan Vaziri, Non-uniform hardening constitutive model for compressible orthotropic materials with application to sandwich plate cores, CMES 10(1) (2005) 79-95.

[63] Ji Hoon Kim, Nyung Gyu Lee, Development of nonlinear constitutive laws for anisotropic and asymmetric fiber reinforced composites, Polymer composites (2008) 216-228.

[64] O.H. Griffin, Jr., M.P. Kamat, Three-Dimensional Inelastic Finite Element Analysis of Laminated Composites, Journal of Composite Materials 15 (1981) 543-560.

[65] Petri Makela, Soren Ostlund, Orthotropic elastic–plastic material model for paper materials, International Journal of Solids and Structures 40 (2003) 5599–5620.

[66] Roland Mucke, Otto-Ernes Bernhardi, A constitutive model for anisotropic materials based on Neuber's rule, Comput. Methods Appl. Mech.Engrg. 192 (2003) 4237-4255.

[67] Ala Tabiei, Jin Wu, Three-dimensional nonlinear orthotropic finite element material model for wood, Composite Structures 50 (2000) 143-149.

[68] Nicholas Metropolis, S. Ulam, The Monte Carlo method, Journal of the American Statistical Association 44 (1949) 335-341.

[69] G. Amaniampong, C.J. Burgoyne, Monte Carlo simulations of the time dependent failure of bundles of parallel fibers, Eur. J. Mech. A/Solids 15(2) (1996) 243-266.

[70] M.E. Cruz, A.T. Patera, A parallel Monte Carlo finite element procedure for the analysis of multicomponent media. Int. J. Num Meth. Engrg. 38 (1995) 1087-1121.

[71] R.L. Iman, W.J. Conover, Small sample sensitivity analysis techniques for computer models, with an application to risk assessment. Communications in Statistics, Part A. Theory and Methods (1980) 1749–1842.

[72] R.E. Melchers, Structural Reliability Analysis and Prediction, John Wiley &, Sons, New York, 2001.

[73] S.S. Isukapalli, A. Roy, P.G. Georgopoulos, Stochastic response surface methods(SRSMs) for uncertainty propagation: Application to environmental and biological systems, Risk Analysis 18(3) (1998) 351-363.

[74] Shuping Huang, Sankaran Mahadevan, Ramesh Rebbaa, Collocation based stochastic finite element analysis for random field problems, Probabilistic engineering mechanics 22 (2007) 194-205.

[75] S. S. Isukapalli, A. Roy, P. G. Georgopoulos, Efficient sensitivity/uncertainty analysis using the combined stochastic response surface method and automated differentiation: Application to environmental and biological systems, Risk Analysis 20(5) (2000) 591-602.

[76] A.A. Henriques, J.M.C. Veiga, J.A.C. Matos, J.M. Delgado, Uncertainty analysis of structural systems by perturbation techniques, Struct. Multidisc. Optim. 35 (2008) 201-212.

[77] S. Sakata, F. Ashida, M. Zako, Kriging-based approximate stochastic homogenization analysis for composite materials, Computa. Methods Appl. Mech. Engrg. 197 (2008) 1953-1964.

[78] Qing-Sheng Yang, Qing-Hua Qin, Micro-mechanical analysis of composite materials by BEM, Engineering Analysis with Boundary Elements 28 (2004) 919-926.

[79] A.A. Henriques, Efficient analysis of structural uncertainty using perturbation techniques, Engineering Structures 30 (2007) 990-1001.

[80] Z. Hashin, S. Shtrikman, A variational approach to the theory of the elastic behavior of polycrystals, J.Mech.Phys.Solids 10 (1962) 343-352.

[81] Anthony Drago, Marek-Jerzy Pindera, Micor-macromechanical analysis of heterogeneous materials: Macroscopically homogeneous vs periodic microstructure, Composite science and technology 67 (2007) 1243-1263.

[82] S. Sakata, F. Ashida, T. Kojima, M. Zako, Three-dimensional stochastic analysis using a perturbationbased homogenization method for elastic properties of composite material considering microscopic uncertainty, International Journal of Solids and Structures 45 (2008) 894–907.

[83] S. Sakata, F. Ashida, M. Zako, Kriging-based approximate stochastic homogenization analysis for composite materials, Comput. Methods Appl. Mech. Engrg. 197 (2008) 1953-1964.

[84] Roger Ghanem, John Red-Horse, Propagation of probabilistic uncertainty in complex physical systems using a stochastic finite element approach, Physica D 133 (1999) 137–144.

[85] D. R. Millman, P. I. King, Estimating the probability of failure of a nonlinear aeroelastic system, Journal of Aircraft 43 (2006) 504-516.

[86] Nicolas Lamorte, Bryan Glaz, Uncertainty propagation in hypersonic aerothermoelastic analysis, 51st AIAA/ASME/ASCE/AHS/ASC Structures, Structural dynamics, and Materials conference,12-15 April 2010, Orlando, Florida

[87] Hamed Haddad Khodaparast, John E. Mottershead, Kenneth J. Badcock, Propagation of structural uncertainty to linear aeroelastic stability, Computers and Structures 88 (2010) 223–236.

[88] Xiaolei Yin, Wei Chen, Albert To, Cahal McVeigh, Wing Kam Liu, Statistical volume element method for predicting microstructure–constitutive property relations, Comput. Methods Appl. Mech. Engrg. 197 (2008) 3516–3529.

[89] Boris Jeremic, Kallol Sett, Probabilistic elasto-plasticity: formulation in 1D, Acta Geotechnica 2 (2007) 197–210.

[90] Maciej Anders, Muneo Hori, Stochastic finite element method for elasto-plastic body, Int. J. Numer. Meth. engng. 46 (1999) 1897-1916.

[91] Maciej Anders, Muneo Hori, Three-dimensional stochastic finite element method for elasto-plastic bodies, Int. J. Numer. Meth. Engng 51 (2001) 449-478.

[92] R.B. McKee, Jr., George Sines, A statistical model for the tensile fracture of parallel fiber composites, J. ELASTOPLASTICS 1 (1969) 185-199.

[93] Jack R. Vison, Robert L. Sierakowski, The behavior of structures composed of composite materials, Kluwer academic publishers, NY, 2004.

[94] Alan Baker, Stuart Dutton and Donald Kelly, Composite materials for aircraft structures, second edition, AIAA, 2004.

[95] William D. Callister, Jr., Materials science and engineering an introduction, John Wiley & Sons, Inc.,2003.

[96] Debdatta Ratna, epoxy composites: Impact resistance and flame retardancy: Rapra Review Reports 185 16(5), 2007.

[97] Derek Hull, T.W. Clyne, An introduction to composite materials, second edition, Cambridge University Press, 1996.

[98] Alan Baker, Stuart Dutton, Donald Kelly, Composite materials for aircraft structures, second edition, AIAA, 2004.

[99] Deborah D.L. Chung, Carbon fiber composite, Butterworth-Heinemann, 1994.

[100] Dassault systems, Abaqus version 6.9 analysis user's manual, 2009.

[101] Bodo Fiedler, Thomas Hobbierunken, Influence of stress state and temperature on the strength of epoxy resins, 11th International conference on fracture, Turin, Italy, March 20-25, 2005.

[102] Jacob Lubliner, Plasticity theory, Dover publication, 2008.

[103] R. von Mises, Mechanik der festen Körper im plastisch deformablen Zustand. Göttin. Nachr. Math. Phys. 1 (1913) 582–592.

[104] R. Hill, A theory of the yielding and plastic flow of anisotropic metals. Proc. Roy. Soc. London 193 (1948) 281–297.

[105] R. Hill, Theoretical plasticity of textured aggregates. Proceedings of the Cambridge Philosophical Society 75 (1979) 179-208.

[106] R. Hill, Constitutive modeling of orthotropic plasticity in sheet metals. Journal of the Mechanics and Physics of Solids 38(3) (1990) 405-417.

[107] R. Hill, Plastic anisotropy and the geometry of yield surfaces in stress space, Journal of the Mechanics and Physics of Solids 48 (2000) 1093-1106.

[108] Walter Ramberg, Willam R. Osgood, Description of stress-strain curves by three parameters, National Advisory Committee for Aeronautics, Technical Note 902,1943.

[109] Sinisa Dj Mesarovic, Jagan Padbidri, Minimal kinematic boundary conditions for simulations of disordered microstructures, Philosophical magazine 85(1) January 2005, 65-78.

[110] S.S. Isukapalli, Uncertainty analysis of transport-transformation models. PhD Thesis, Rutgers University, Piscataway, NJ. 1999.

[111] R. H. Myers, D. C. Montgomery, Response surface methodology, Wiley, New York, 1995.

[112] W. Gautschi, Orthogonal Polynomials: Applications and computations. Acta Numerica 5 (1996) 45-119.

[113] D. Xiu, D. Lucor, C.H. Su, G.E. Karniadakis, Stochastic modeling of flow-structure interactions using generalized polynomial chaos, Journal of Fluids Engineering 124(1) (2002) 51-59.

[114] Sastry S. Isukapulli, Panos G.Georgopoulos, Computationally efficient uncertainty propagation and reduction using the stochastic response surface method, 43rd IEEE Conference on Decision and Control, December 14-17, 2004.

[115] A.A. Henriques, J.M.C. Veiga, J.A.C. Matos, J.M. Delgado, Uncertainty analysis of structural systems by perturbation techniques, Struct. Multidisc. Optim. 35 (2008) 201-212.

[116] M.D. Webster, M.A. Tatang, G.J. McRae, Application of the probabilistic collocation method for an uncertainty analysis of a simple ocean model, MIT Joint Program on the Science and Policy of Global Change, 1996.

[117] J. Villadsen, M.L. Michelsen, Solution of differential equation models by polynomial approximation, Prentice Hall, Englewood Cliffs, New Jersey, 1978.

BIOGRAPHICAL SKETCH

Jinuk Kim was born in Pusan, South Korea (Republic of Korea) in 1972. He received a Bachelor of Science and Master of Science in mechanical engineering from Sungkyunkwan University in Korea in March 2000. He worked as an intern researcher in SAFE research center in Sungkyunkwan University until 2002 studying on Tribology. At the University of Michigan, he earned a Master of Science in mechanical engineering and a Master of Science in materials science and engineering in July 2006. For further study, he went to the University of Florida to pursue a Ph.D. degree in materials science and engineering where he earned his doctorate in August 2011.